2017

The islet-resident macrophage is in an inflammatory state and senses microbial products in blood

Stephen T. Ferris
Washington University School of Medicine in St. Louis

Pavel N. Zakharov
Washington University School of Medicine in St. Louis

Xiaoxiao Wan
Washington University School of Medicine in St. Louis

Boris Calderon
Washington University School of Medicine in St. Louis

Maxim N. Artyomov
Washington University School of Medicine in St. Louis

See next page for additional authors

Recommended Citation

Authors

Stephen T. Ferris, Pavel N. Zakharov, Xiaoxiao Wan, Boris Calderon, Maxim N. Artyomov, Emil R. Unanue, and Javier A. Carrero

The islet-resident macrophage is in an inflammatory state and senses microbial products in blood

Stephen T. Ferris,* Pavel N. Zakharov,* Xiaoxiao Wan, Boris Calderon, Maxim N. Artyomov, Emil R. Unanue, and Javier A. Carrero

Department of Pathology and Immunology, Washington University School of Medicine, St. Louis, MO

We examined the transcriptional profiles of macrophages that reside in the islets of Langerhans of 3–wk–old non–obese diabetic (NOD), NOD.*Rag1*^{−/−}, and B6.g7 mice. Islet macrophages expressed an activation signature with high expression of *Tnf*, *Il1b*, and MHC-II at both the transcript and protein levels. These features are common with barrier macrophages of the lung and gastrointestinal tract. Moreover, injection of lipopolysaccharide induced rapid inflammatory gene expression, indicating that blood stimulants are accessible to the macrophages and that these macrophages can sense them. In NOD mice, the auto-immune process imparted an increased inflammatory signature, including elevated expression of chemokines and chemokine receptors and an oxidative response. The elevated inflammatory signature indicates that the autoimmune program was active at the time of weaning. Thus, the macrophages of the islets of Langerhans are poised to mount an immune response even at steady state, while the presence of the adaptive immune system elevates their activation state.

INTRODUCTION

An emerging theme in macrophage biology is that each tissue macrophage is adapted to its local environment and provides homeostatic support (Amit et al., 2016). Although all the tissue macrophages share core gene transcripts, including the transcription factor *Spi1* (PU.1) and cell surface receptors such as *Mertk* (Mer) and *Fcgr1* (CD64), a comparison of different organs reveals substantial differences that may relate to a specific function (Gautier et al., 2012). Macrophages share a common set of enhancers, but these are differentially expressed in a tissue-specific manner, leading to their specialization (Kaikkonen et al., 2013; Lavin et al., 2014). For example, red pulp macrophages are specialized to dispose of effete red blood cells by sensing heme and inducing *Spic* (Haldar et al., 2014). Understanding how the phenotypic qualities of many tissue macrophages originate and are influenced by their surrounding tissues is a work in progress.

The pancreas contains distinct resident macrophages in the exocrine and endocrine regions (Calderon et al., 2015). In each anatomical site, the macrophages differ in their embryonal origin and in their activation status. In an analysis performed in C57BL/6 mice, the interacinar macrophages were found to express genes and cell surface markers that categorize them as M2-like (anti-inflammatory) and tissue supportive. In contrast, the macrophages in the islets of Langerhans expressed M1-like transcripts typically associated with inflammatory macrophages. The islet macrophage has a ho-

meostatic role, as shown in the *op/op* mouse, which lacks functional CSF-1 protein. In these mice, the islets lack macrophages and develop poorly (Banaei-Bouchareb et al., 2004; Calderon et al., 2008, 2015). Also, the islet macrophages are intimately associated with intra-islet vessels and in close contact with β cells (Calderon et al., 2011). Islet macrophages take up dense core granules and can present the contents of the islet granule to islet reactive CD4^{+} T cells (Vomund et al., 2015).

There has been confusion in the field about the identity of tissue-resident macrophages and DCs. The main reason has been the long-standing assumption that expression of CD11c and high MHC-II were specific markers of DCs and that high F4/80 was a signature of the macrophage. In fact, CD11c and MHC-II expression are not definitive markers, many tissue-resident macrophages express CD11c and MHC-II, and F4/80 levels vary across the macrophage lineage. Recent data have identified more faithful markers for both cells. In the case of macrophages, the cell surface receptors MerTK and FcγRI are among the most reliable markers (Gautier et al., 2012). In the case of DCs, the conventional DCs are best defined by a group of genes that includes *Zbtb46* and *Flt3*, while the plasmacytoid DC (pDC) lineage is best defined by expression of B220, PDCA, and SiglecH (Miller et al., 2012). The islet macrophages are positive for expression of canonical macrophage proteins or genes such as MerTK, FcγRI, and *Sfpi1* but do not express the DC markers *Zbtb46*, *Flt3*, B220, and Siglec H (Ferris et al., 2014; Calderon et al., 2015).

Comparing the islet macrophages from nondiabetic mice with early prediabetic mice is important. The macro-

Supplemental material can be found at:
http://doi.org/10.1084/jem.20170074

Check for updates

phages constitute the majority of the leukocytes found in islets at steady state, and they can act as a potential modulator of T cell activation in vivo. Our studies therefore focus on the 3-wk-old mouse, a time before there is overt lymphocytic infiltration of islets. Overall, the role of the macrophage in the autoimmune diabetic process is not well understood. In the non–obese diabetic (NOD) mouse, a strain that develops spontaneous diabetes, the first inflammatory transcriptional signatures that can be detected can be mapped back to myeloid cells generally and macrophages specifically (Carrero et al., 2013). At this early stage in NOD diabetogenesis, a second myeloid cell, the *Batf3*-dependent XCR1+ DC, enters the islets, but the relationship between the two cells is not known. The importance of myeloid cells in diabetogenesis is reinforced by the finding that the NOD.*Batf3*−/− mice lacking XCR1+ DCs never develop diabetes (Ferris et al., 2014).

Islet macrophages from two strains of nondiabetic mice were in an activated state comparable with other barrier macrophages, such as those found within the lung and the intestine. They expressed high MHC-II, TNF, and IL-1β, all at the transcript and protein level, as well as a host of other inflammatory mediators and sensors. Importantly, the islet macrophages are sampling blood contents, as there was increased expression of inflammatory transcripts after treatment with intravenous LPS. In the NOD mouse, the islet macrophage was sensitive to the presence of an adaptive immune system, having an increased expression of inflammatory transcripts. Interferon-inducible gene signatures were identified in macrophages from 3-wk-old NOD mice, clearly indicating that the diabetic process was already under way very early in the life of the mouse. Finally, in a deeper analysis of the islet macrophages, a quarter of the NOD macrophages had increased inflammatory transcripts, higher than those found in the basal state.

RESULTS

Core features of the NOD, NOD.*Rag1*−/−, and B6.g7 islet–resident macrophages

We isolated 3-wk-old islet macrophages (CD45+F4/80+MHC-II+) using the gating strategy shown in Fig. S1 A. Note that 85–95% of the CD45+ cells in the islets of the 3-wk-old NOD mice are macrophages; the remaining cells are mostly CD3ε+ T cells (see also Melli et al., 2009). (Previous work showed that islets at 3 wk or earlier contained B cells, neutrophils, and pDCs [Diana et al., 2013; Diana and Lehuen, 2014]. However, our experimental analysis did not reproduce these findings [Figs. S2 and S3].)

We compared macrophages isolated from NOD, NOD.*Rag1*−/−, and B6.g7 mice pancreatic islets for their gene expression profiles by RNA sequencing (RNASeq) and cell surface marker expression. Examination of the NOD.*Rag1*−/− and B6.g7 mice established their basal features independent of autoimmune inflammation. All mice used in this study were housed in an advanced pathogen-free barrier facility, developed normally, and did not have any indication of infections.

We also included lung macrophages and pancreatic LN (PLN) XCR1+ DCs (CD45+CD11c+MHC-II+CD172aneg CD11bnegXCR1+) for additional comparisons (Fig. S1, B and C). A preliminary analysis of the islet macrophage data using the Immunological Genome Project (ImmGen) My GeneSet tool showed that the lung and intestinal macrophages most closely resembled those of the islet (Heng et al., 2008). We chose the lung macrophage to determine both common and unique gene expression signatures of the islet macrophage when compared with other tissue macrophages. (There are two annotated lung macrophages in ImmGen: the "lung CD11b+ macrophage" that is CD11bhiCD11c+MHC-II+CD103negCD24neg and the "lung macrophage" that is CD11c+MHC-IInegCD11bnegCD103negSiglecF+. Our preliminary analysis showed high similarity between the islet macrophage and the "lung CD11b+ macrophage," leading us to examine that population.) The XCR1+ DCs represent a different phagocyte lineage that is highly relevant for the initiation of diabetes (Ferris et al., 2014). The absence/paucity of these DCs in islets at the 3-wk window made it difficult to analyze them, so instead we isolated them from the PLN on the basis of their expression of XCR1. This combination of tissues and cell types allowed us to interrogate several questions about the transcriptional profile and biology of the islet macrophage.

The top expressed transcripts in 3-wk-old islet macrophages showed similar values (Fig. 1, A–C). Housekeeping genes, such as transcriptional regulators and cell structural genes (i.e., *Actb*, *Fosb*, and *Hspa5*), were comparably expressed (Fig. 1 A and Table S1). Most canonical myeloid genes were comparably transcribed in both islet macrophages and in PLN DCs (Fig. 1 B; Gautier et al., 2012). Included in this group were the MHC-II antigen presentation genes *H2-Aa*, *H2-Ab1*, *H2-Eb1*, and *Cd74*. The islet macrophages do not initially express uniformly high MHC-II on their surface (Calderon et al., 2015). At 2 wk of age, they have varying levels of MHC-II on their surface. However, by 4 wk of age, MHC-II expression becomes uniformly high (Fig. S1 D). Unlike DCs, high expression of MHC-II genes is not a basal condition in all tissue-resident macrophages. Microglia, the large peritoneal macrophages, and alveolar macrophages express low levels of MHC-II genes and the master regulator *Ciita* (Fig. S1 E shows data from ImmGen).

Three additional classes of genes integral to the initiation of an adaptive immune response were expressed highly in islet macrophages: (1) costimulatory molecules, (2) pattern recognition molecules (TLRs), and (3) chemokines (Fig. 1, D–G). (1) The most notable costimulatory genes were the activating ligands *Cd86* and *Pvr* (CD155) and the inhibitory ligands *Lgals9* (Galectin-9) and *Cd274* (PD-L1; Fig. 1 D). (2) Most TLR genes and adaptor proteins were expressed at high levels, including *Tlr1*, *Tlr2*, *Tlr3*, *Tlr4*, *Tlr6*, *Tlr7*, *Tlr8*, *Tlr9*, *Tlr12*, and *Tlr13*, allowing the islet macrophages to sense different microbial patterns (Fig. 1 E; Kawai and Akira, 2011; Oldenburg et al., 2012; Koblansky
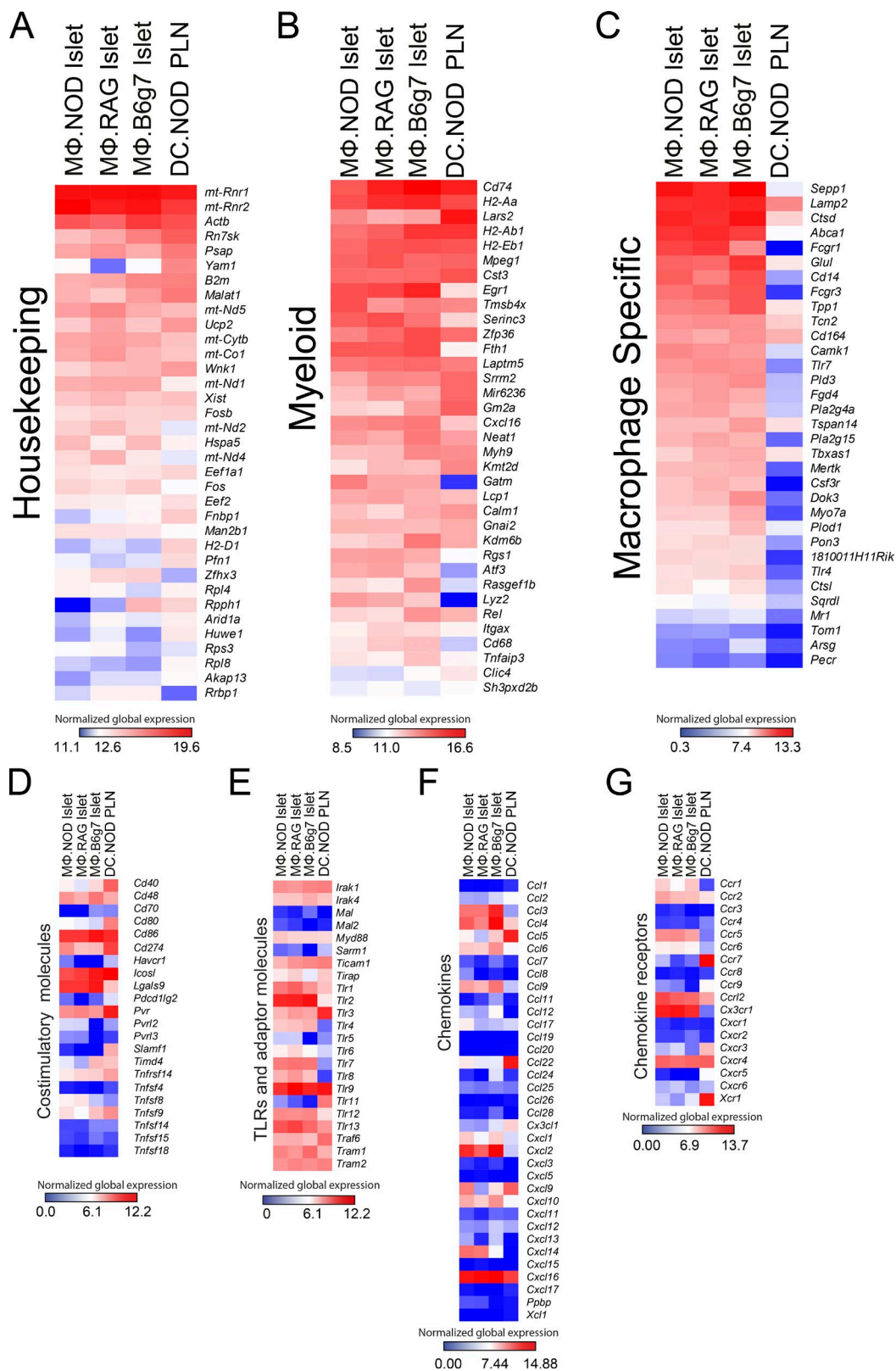
Figure 1. Transcriptional profiling of islet–resident macrophages. Top expressed housekeeping (A) and myeloid (B) genes from NOD, NOD.$Rag1^{-/-}$, and B6.g7 islet macrophages and DCs. Macrophages and DCs were isolated as indicated in Fig. S1. (C) Core macrophage-specific gene signature (as defined by Gautier et al., 2012), distinguishing macrophages from DCs. Expression of costimulatory genes (D), genes encoding TLRs and adaptors (E), chemokines (F),

et al., 2013). In contrast, the XCR1+ DCs had reduced or absent expression of most of the TLRs, except *Tlr3*, *Tlr9*, and *Tlr11*. (3) Chemokine expression consisted of genes capable of attracting myeloid cells (*Ccl3*, *Cxcl14*), macrophages (*Ccl9*, *Cxcl14*), neutrophils (*Cxcl1*, *Cxcl2*), NK cells (*Ccl3*), NKT cells (*Cxcl16*), T cells (*Ccl4*, *Cxcl9*, *Cxcl10*, *Cxcl16*) and regulatory T cells (*Cxcl9*; Fig. 1 F; Matloubian et al., 2000; Kurth et al., 2001; Dufour et al., 2002; Zhao et al., 2003; Castellino et al., 2006; Yamada et al., 2012; Griffith et al., 2014). Finally, islet macrophages expressed chemokine receptors found in inflammatory leukocytes (*Ccr2*, *Ccr5*), developing leukocytes (*Cxcr4*), barrier macrophages (*Ccr2*, *Ccr5*, *Ccrl2*, *Cx3cr1*, *Cxcr4*), and microglia (*Cx3cr1*) but whose combined pattern of expression most resembled barrier macrophages (Fig. 1 G; Gautier et al., 2012; Griffith et al., 2014).

Several myeloid genes were differentially expressed in the islet macrophages compared with the PLN DCs. Among these were *Atf3*, *Rasgef1b*, and *Rgs1* (Fig. 1 B). *Atf3* is downstream of TLR4 signaling and acts as a negative regulator of cytokine transcript expression after LPS treatment (Gilchrist et al., 2006). *Rasgef1b* encodes a guanine-nucleotide exchange factor induced by TLR signaling and believed to activate Ras-like proteins (Andrade et al., 2010). *Rgs1* encodes a regulator of G-protein-coupled signaling that antagonizes chemokine receptor signaling (Reif and Cyster, 2000; Moratz et al., 2004). Genome-wide association studies have linked *Rgs1* to celiac disease and type 1 diabetes, but its exact function in autoimmunity is poorly defined (Smyth et al., 2008). All three of these genes (*Atf3*, *Rasgef1b*, and *Rgs1*) are also highly expressed in lung and intestinal macrophage (Heng et al., 2008).

For validation purposes, we identified several cell surface receptors using the Panther classification system (Mi et al., 2013, 2016). In this way, CD44, CD53, CD83, and TLR-7 were identified and validated by flow cytometry, as shown in Fig. S1 F.

NOD islet macrophages expressed higher levels of inflammatory transcripts than NOD.*Rag1*−/− at 3 wk of age

We compared the gene expression profiles of the NOD, NOD.*Rag1*−/−, and B6.g7 islet macrophages, the CD11b+ lung macrophage, and the XCR1+ DC. Principal component analysis (PCA), based on the top 5% of gene expression variance, clustered the islet macrophages tightly along the first and second components and related them more closely to the CD11b+ lung macrophage than to the PLN XCR1+ DCs (Fig. 2 A). Pearson correlation and hierarchical clustering reinforced this point, demonstrating the similarity between NOD, NOD.*Rag1*−/−, and B6.g7 macrophages (Fig. 2, B and C).

The NOD macrophage at 3 wk contained an activation signature when compared with the NOD.*Rag1*−/− macrophage. Using DESeq2, we found 542 genes differentially expressed at twofold counts (adjusted $P \leq 0.05$; Fig. 2, D and E). Of these, 314 were up-regulated in NOD and 228 were up-regulated in NOD.*Rag1*−/− (Fig. 2 D).

By hypergeometric analysis, the major Gene Ontology (GO) pathways enriched in NOD-up-regulated genes mapped to signal transduction, cellular biosynthetic process, inflammatory response, response to external stimulus, and defense response (Fig. 2 F). The top C2 pathways (curated gene sets) enriched in NOD macrophages mapped to KEGG oxidative phosphorylation, KEGG Huntington's disease, Naba matrisome associated, and KEGG cytokine/cytokine receptor interaction (Fig. 2 F; Kanehisa and Goto, 2000; Mootha et al., 2003).

We performed gene set enrichment analysis (GSEA) using Broad Institute software (Subramanian et al., 2005), and this revealed a correlation of the NOD-up-regulated genes with the GO MSigDB biological process gene signatures that associate with oxidative phosphorylation, inflammation, cellular response to reactive oxygen species (ROS), and cell proliferation (Fig. 2 G; $P < 0.002$ and false discovery rate [FDR] q < 0.05: response to oxidative stress [GO term: 0006979], behavior [GO term: 0007610], and inflammatory response [GO term: 0006954]).

These findings show that the NOD macrophages are transcriptionally and metabolically more active than their NOD.*Rag1*−/− counterparts. First, the behavior and inflammatory response grouping contained NOD-up-regulated genes involved in chemotaxis, including the chemokine receptors *Ccr1* and *Ccr7* as well as the chemokines *Ccl5*, *Cxcl2*, and *Cxcl9* (Fig. 2, H and I). Second, the islet macrophages displayed an up-regulation of interferon-inducible genes, including *Cxcl9* and *Ccl5*, along with early innate immune mediators such as *Cd40* (Fig. 2, H and I). A majority of these genes are associated with pathogen-associated molecular pattern signaling and are discussed in greater detail in a later section. Third, the response to oxidative stress signature contained up-regulated genes encoding proteins with an antioxidant role in cells (Fig. 2 J). For example, *Sod1* encodes superoxide dismutase 1, one of two enzymes responsible for converting superoxide radicals to molecular oxygen and hydrogen peroxide (Fridovich, 1995). *Prdx2* and *Prdx5* encode peroxiredoxin 2 and peroxiredoxin 5 antioxidant enzymes, which reduce hydrogen peroxide and alkyl hydroperoxides (Wood et al., 2003). Finally, the oxidative phosphorylation gene signature contained genes whose products are components of the four major complexes of the mitochondrial electron transport chain as well as the ATP synthase complex

and chemokine receptors (G) by islet macrophages and PLN DCs. Costimulatory gene selection was based on Chen and Flies (2013). TLR and TLR adaptors were based on Chevrier et al. (2011). Chemokines and chemokine receptors were based on Griffith et al. (2014). Data are the mean of three or four samples per group and are represented as the $\log_2$ global expression level.
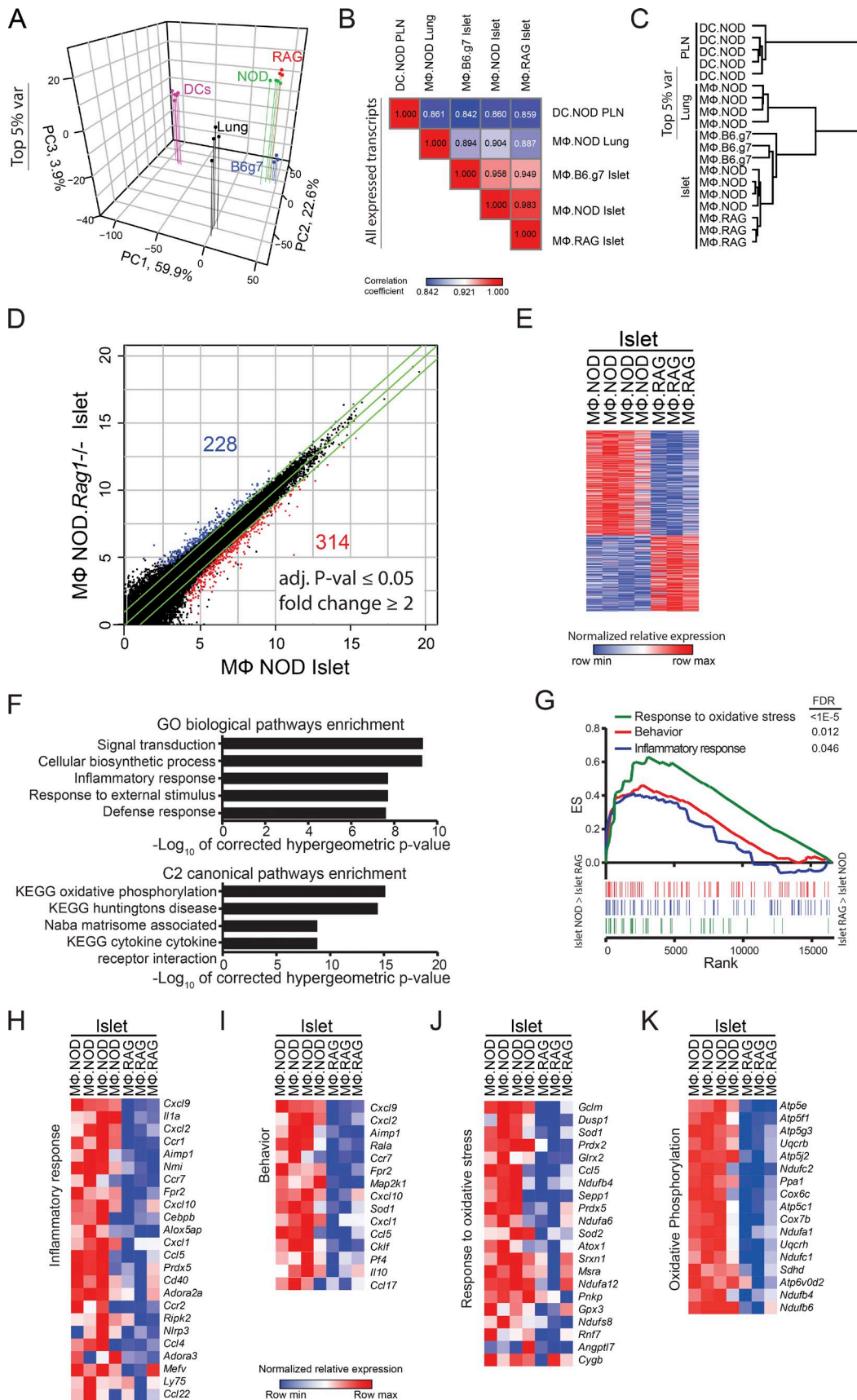
(Fig. 2 K). Combined, these findings point to an increase in the oxidative activity of the NOD macrophages compared with those of the NOD.*Rag1*$^{-/-}$ macrophages.

NOD macrophages at 3 wk of age already display transcriptional signatures of diabetes progression

We examined whether transcripts found during diabetes progression might be up-regulated in the 3-wk-old NOD macrophage (Fig. 3 A). We did this by comparing the islet macrophage transcriptional signature to our previous chronological analysis of whole islets in NOD diabetes (Carrero et al., 2013). Our previous dataset contains the whole-islet transcriptional analysis of type 1 diabetes progression in the NOD mouse from 2 wk of age until the onset of diabetes (∼20–30 wk). This dataset also included control samples from mice that never developed diabetes: B6.g7, C57BL/6, and NOD.*Rag1*$^{-/-}$. We calculated Pearson's correlation of whole-islet transcriptomes on the basis of the transcripts differentially up-regulated in NOD macrophages (the 314 genes described in Fig. 2, D and E; adjusted P ≤ 0.05 and maximum likelihood estimate–adjusted fold change ≥2). Those same 314 genes were used to calculate Pearson's correlation between whole-islet transcriptomes that ranged between 2 wk of age and diabetic onset. We found a gradually increasing and positive correlation from 2 wk to diabetic onset (Fig. 3 A and Fig. S4 A).

The up-regulated transcripts parsed into two clusters that showed significant enrichment in the MSigDB Canonical (C2) and GO biological pathways (C5BP) databases (Fig. 3 B). Cluster I included genes that are progressively up-regulated during NOD diabetes (e.g., *Cxcl9*, *S100a4*, and *Ptgs2*). These were enriched by hypergeometric test for inflammatory pathways, namely, defense response, immune system process, and cytokine/cytokine receptor interaction (Fig. 3 C and Fig. S4 B). Cluster II, in contrast, consisted of genes enriched in developmental pathways, such as cellular biosynthetic process, translation, and oxidative phosphorylation. These genes were up-regulated in the islets of 2-wk-old mice and recently diabetic NOD mice (Fig. 3, B and D; and Fig. S4 C). These transcripts indicate increased cellular activity, likely accountable by some level of replication.

Inflammatory transcripts in the islet macrophage are the hallmark features of a barrier macrophage

GSEA of the genes differentially expressed between NOD and NOD.*Rag1*$^{-/-}$ (Fig. 2 G) revealed a correlation with gene signatures identified in cultured bone marrow–derived macrophages treated with LPS (dataset: GSE14769 samples, unstimulated vs. 40-min LPS bone marrow–derived macrophages dominant-negative (Litvak et al., 2009). Similar findings were made interrogating datasets from macrophages treated with different inflammatory stimuli. In total, we found a significant enrichment score for genes expressed after LPS, TNF, and IL-1 treatment of macrophages (Fig. 4 A).

When further compared with ImmGen datasets, the macrophages that displayed genes up-regulated in an LPS signature were all barrier macrophages and exposed to either intestinal or airborne stimuli. This association was revealed both by hierarchical clustering (Fig. 4 B) and by correlation analysis. Both techniques grouped the intestinal and CD11b$^+$ lung macrophages together and showed that barrier macrophages as a group had a higher enrichment score for LPS signatures than the nonbarrier macrophages (Fig. S4 D).

Gene signatures induced by LPS, TNF, and IL-1 were found highest in the CD11b$^+$ lung macrophage, NOD, NOD.*Rag1*$^{-/-}$, and B6.g7 islet macrophages but not in the bone marrow macrophage (Fig. 4, C and D). This indicated that at steady state, the islet macrophages were in an activated state comparable with those at a barrier surface.

The similarities between the islet-resident macrophage and barrier macrophages led us to compare our own gene expression profiles between the islet and the CD11b$^+$ lung macrophage to identify islet macrophage–enriched signatures. The top statistically significant canonical signature by GSEA that distinguished the islet macrophage from the CD11b$^+$ lung macrophage was lysosome (FDR < 1.0E-5, P < 1.0E-5; Fig. 4, E and F). The lysosome signature included genes encoding eight cathepsins (A/B/C/D/H/O/S/Z), *Laptm4b*, *Laptm4a* (lysosomal protein transmembrane 4 alpha and beta), and *Lgmn* (legumain cysteine protease). This gene signature suggested a higher lysosomal activity in the islet macrophages than in the CD11b$^+$ lung macrophages (Fig. 4 F; Ewald et al., 2011). The lysosomal gene signature was found in all islet datasets, indicating that heightened lysosomal function was a steady-state feature of islet macrophages.

Figure 2. **Analysis of islet macrophage transcriptional diversity.** (A) PCA of the 5% of genes with the greatest variability for XCR1$^+$ DCs, NOD CD11b$^+$ lung macrophages, and NOD, NOD.*Rag1*$^{-/-}$, and B6.g7 islet macrophages. (B) Pearson's correlation matrix of macrophages and DCs on the basis of all expressed RNASeq probes. (C) Hierarchical clustering of macrophages and DCs for the top 5% of genes with the greatest variability. (D) Scatterplots of expression values of all annotated genes. (E) Heat map of differentially expressed genes taken from D. Each dot represents the mean of four independent biological replicates for NOD and three for NOD.*Rag1*$^{-/-}$ conditions. Numbers in plots indicate probes with a DESeq2-calculated fold change between conditions of ≥2 and adjusted P ≤ 0.05 at an FDR of 5% (red, up-regulated in NOD; blue, up-regulated in NOD.*Rag1*$^{-/-}$). (F) GO and canonical (C2) pathway hypergeometric analysis of the genes differentially expressed between NOD and NOD.*Rag1*$^{-/-}$ islet macrophages. (G) Enrichment plots from GSEA analysis performed on differentially expressed genes using GO biological process (MSigDB C5BP) signature gene sets. ES, enrichment score. Heat maps of core enrichment genes from "inflammatory response" (H), "behavior" (I), "response to oxidative stress" (J), and "oxidative phosphorylation" (K) gene sets, identified by either GO (F) or GSEA (G). Heat maps show individual samples and represent the log$_2$ row normalized expression.
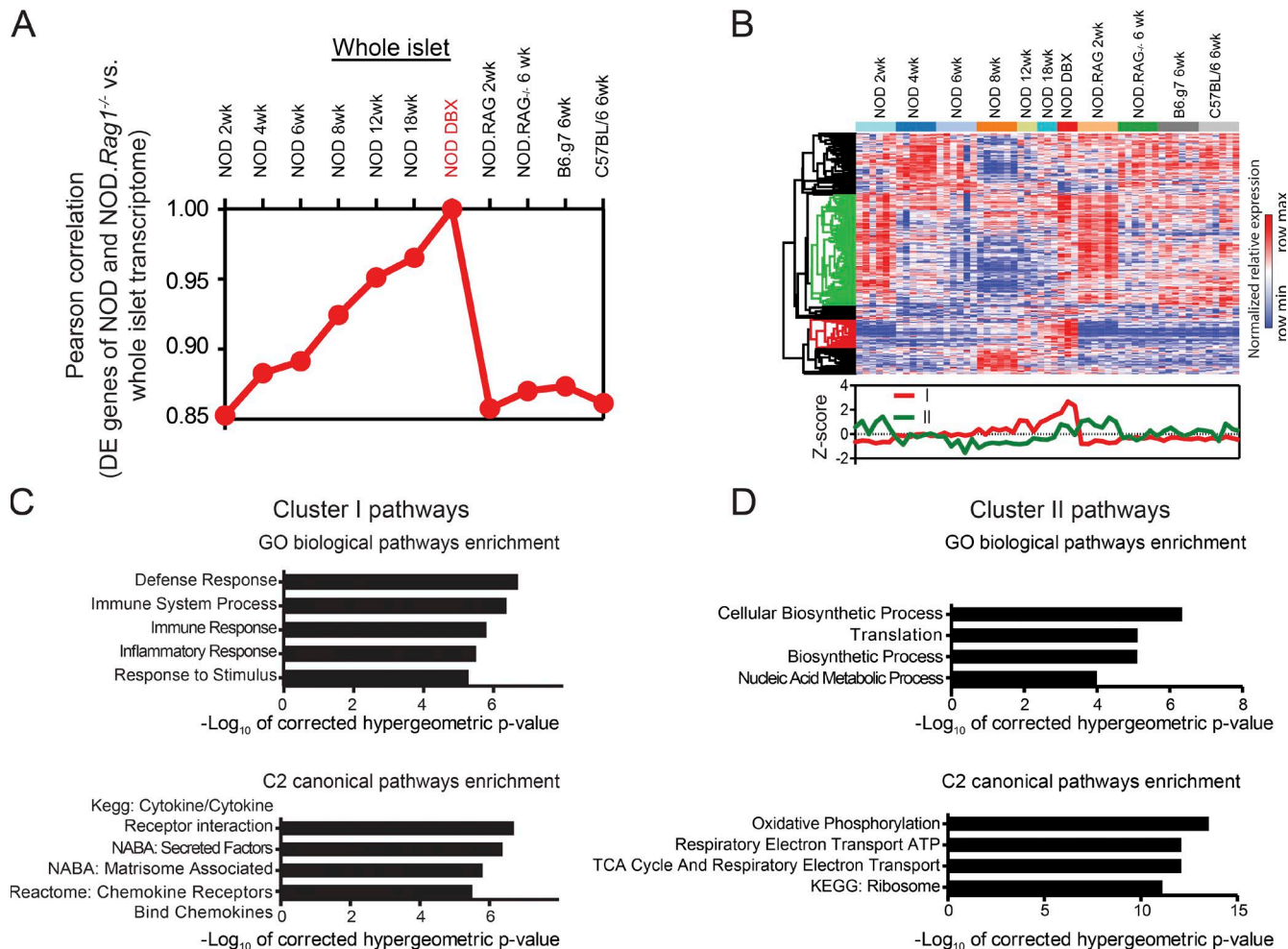
Figure 3. **Early inflammatory signature during diabetogenesis.** (A) Pearson's correlation of samples from Carrero et al. (2013) on the basis of genes identified using DESeq2 as differentially up-regulated in NOD versus NOD.*Rag1*^{−/−} macrophages with adjusted P ≤ 0.05 and fold change ≥2. (B) Hierarchically clustered genes from A in whole-islet transcriptome analysis (top). The Z-score profiles of genes expression in cluster I (red) and cluster II (green) are shown (bottom). Sample number ranged from three to six per group. Each column represents data obtained from one biological replicate each composed of all the intact islets isolated from one mouse of the indicated genotype. (C and D) Hypergeometric analysis of the genes identified in clusters I and II in B using GO biological pathways and C2 canonical pathways.

Inflammatory mediator production by the islet macrophages

Intracellular flow cytometry showed production of IL-1β and TNF, confirming the RNASeq analysis (Fig. 5 A). About half of the NOD.*Rag1*^{−/−} islet macrophages were producing detectable levels of TNF and IL-1β without any stimulation. Activation with PMA and ionomycin led to limited increases in TNF and IL-1β proteins, revealing that they were at or near maximal production (Fig. 5, A and B). For comparison, the CD11b^{+} lung macrophage produced almost no detectable TNF but equivalent IL-1β (Fig. 5, A and B). Even when pulsed with PMA/ionomycin, CD11b^{+} lung macrophage TNF cytokine production never reached that of steady-state islet macrophage levels (Fig. 5 B). Their production of IL-1β protein was equivalent to the islet macrophages and did not increase when pulsed with PMA/ionomycin (Fig. 5, A and B).

Activation of IL-1β from its pro form to its active form requires processing by an active inflammasome-family caspase (Dinarello, 2009). Islet macrophages from NOD and NOD.*Rag1*^{−/−} expressed a detectable level of active caspase-1 when examined with the fluorescent form of the caspase substrate YVAD. The CD45-negative fraction (i.e., the endocrine cells) was negative (Fig. 6 A).

The data indicate that the islet macrophages are making some level of both active IL-1β and TNF. Because both receptors converge on the NF-κB pathway, we analyzed our transcriptional data, searching for NF-κB family members expressed in the whole islet. The only members of the transcription factors and coactivators contained in the NF-κB and Rel family detectable above background were *Nfkb1* (p105/p50) and *Rela* (p65; Carrero et al., 2013). Therefore,
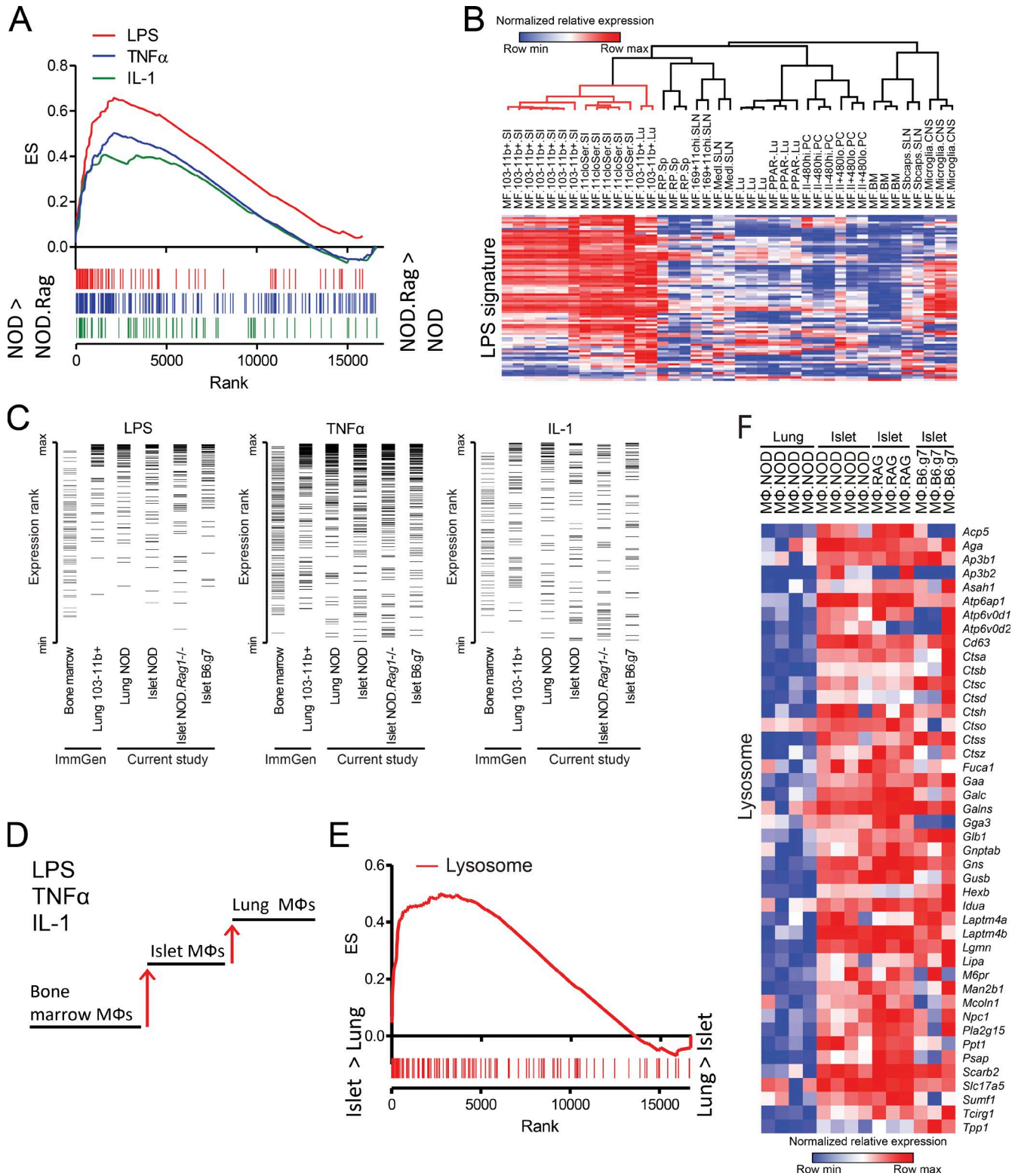
Figure 4. Islet macrophages are similar to barrier macrophages. (A) GSEA enrichment plots of NOD versus NOD.*Rag1*^{−/−} islet macrophage differences on the basis of LPS, TNF, and IL-1 signatures. The differences between NOD and NOD.*Rag1*^{−/−} were compared with published signatures of LPS, TNF, and IL-1 cells as described in Materials and methods. ES, enrichment score. (B) Hierarchical clustering of ImmGen microarray data for macrophages from different tissues. The LPS signature genes were selected for clustering the macrophage microarray data from ImmGen. Heat map shows the log$_2$ row normalized expression. (C) LPS, TNF, and IL-1 signatures from bone marrow and lung (CD103^{neg}CD11b^{+}) macrophage microarrays (ImmGen), and lung and islet macro-

we examined the nuclear localization of the NF-κB component RelA/p65 (Rütti et al., 2016). Staining for RelA/p65 revealed a predominantly cytosolic pattern of staining in NOD islets at 6 wk of age (Fig. 6 B, top). As a positive control, islet cells treated with IL-1β induced nuclear localization (Fig. 6 B, bottom). Therefore, despite the expression of IL-1β and TNF by islet macrophages, there was limited detectable nuclear NF-κB in the endocrine pancreas. These data indicate that despite the levels of cytokine being made by the islet macrophages, the β cells are not strongly signaling.

Islet macrophages respond to blood–borne stimuli
A blood-borne stimulus might be able to induce part of activation profile in the macrophage, as suggested by the expression of *Tnf*, *Il1a*, and *Il1b* transcripts. This idea is supported by our previous finding that the islet macrophage extended filopodia into the lumen of the blood vessel and could interact with blood-borne particles (Calderon et al., 2011).

To determine if a blood-borne TLR–agonist could stimulate the islet macrophage, we injected LPS at low concentrations that would not induce systemic effects. LPS was injected intravenously into 3–wk-old NOD and NOD.$Rag1^{-/-}$ mice. Islets were isolated 3 h later, and the islet macrophage was sorted using the strategy outlined in Fig. S1. Transcripts associated with signaling of TLR4 were assayed using quantitative RT-PCR (qRT-PCR). The transcripts for *Cxcl9*, *Ccl5*, *Il12b*, *Nos2*, and *Il6* were significantly up-regulated after LPS injection of NOD.$Rag1^{-/-}$ mice when compared with control PBS-injected mice (Fig. 6 C). *Cxcl9*, *Ccl5*, and *Il12b* were up-regulated in the NOD mice. Notably, the NOD mice displayed higher baseline expression than the NOD.$Rag1^{-/-}$ mice for all markers examined. This was not surprising, as some of these markers were the most differentially expressed between NOD and NOD.$Rag1^{-/-}$ mice by RNA-Seq (Fig. 2 D). In sum, the islet macrophage is accessible and reacting to circulating LPS, a strong representative pathogen–associated molecular pattern.

Single–cell analysis of islet macrophages reveals heterogeneity in the NOD but not the NOD.$Rag1^{-/-}$ mice
We examined if the inflammatory gene expression differences between NOD and NOD.$Rag1^{-/-}$ islets was due to homogeneous or heterogeneous autoimmune activation of the NOD macrophages. To interrogate transcriptional heterogeneity at the cellular level, we examined individual macrophages from NOD and NOD.$Rag1^{-/-}$ islets. Macrophages were sorted directly into RNA lysis buffer, cDNA was synthesized and preamplified, and qRT-PCR was performed for 95 different markers using the Fluidigm Biomark HD system. The starting

cell inputs were 184 NOD and 95 NOD.$Rag1^{-/-}$ macrophages. After outlier detection using Singular analysis software, 143 NOD and 79 NOD.$Rag1^{-/-}$ macrophages were kept for further analysis.

By PCA, the majority of macrophages from both mice clustered together, except for a subset in the NOD samples represented by 42 of 184 (22.8%; outlined in Fig. 7 A). The combination of ANOVA and fold change analysis was performed on the normalized expression values (log$_2$ex) of the single macrophage PCR data (Fig. 7 B). We identified several genes previously shown to be differentially expressed between NOD and NOD.$Rag1^{-/-}$ samples by RNASeq, including *Ccl5*, *Cxcl9*, *Ly6a*, *Cd38*, and *Dnase1l3*. However, *Cxcl9* was the most significant differentially expressed gene. All of the cells contained in the NOD outlier population expressed high levels of *Cxcl9*. The population level macrophage RNASeq data showed that *Cxcl9* was the most differentially expressed gene between the NOD and NOD.$Rag1^{-/-}$ samples, and the expression of this chemokine was detected only in the NOD outlier population (Fig. 2 D and 7 A and Table S1). In total, 26 of 95 genes interrogated by single cell qRT-PCR were differentially expressed between NOD and NOD.$Rag1^{-/-}$ samples at twofold change and P < 0.01. Selection of these genes revealed a cluster enriched in only NOD but not NOD.$Rag1^{-/-}$ samples (Fig. S5 A, left side of the heat map; for the heat map of the entire dataset, see Fig. S5 B).

In brief, the islet-resident macrophages in the NOD.$Rag1^{-/-}$ mouse were homogeneous. In the NOD mouse at 3 wk, there was heterogeneity in their activation state. There was a major set identical to the NOD.$Rag1^{-/-}$ macrophage but also a second that expressed the same up-regulated transcripts revealed by the RNASeq analysis.

DISCUSSION
We made three key findings that place the resident macrophage in a unique position to regulate islet function. First, the islet macrophages are in an activated state comparable with macrophages exposed at barrier surfaces. This result leads to the obvious question: why are these macrophages in such a state? The islet is a mini-organ that is constantly responding to several stimuli that vary and oscillate, such as blood glucose, the most prevalent bioactive molecule. We have reported that the macrophages capture dense core granules and therefore must be exposed to the products of the β cell (Vomund et al., 2015). We also showed here how blood products, in our example a low dose of LPS, were accessible to the islet macrophage. In a previous paper, we indicated that the islet macrophages extended filopodia into the blood vessel lumen, which could be the interacting structure with the circulation (Calderon et

phages from the present study. All expressed genes were ranked by expression level, and genes that match to the signatures are depicted as horizontal lines. (D) Schematic illustration of expression levels of the LPS, TNF, and IL-1 signatures genes in different macrophages. (E) GSEA enrichment plot of the lysosome gene pathway, the top canonical (C2, MSigDB) pathway up-regulated in islet macrophages when compared with CD11b+ lung macrophages. (F) Heat map of the core enrichment genes from E. Heat map shows individual samples and represent the log$_2$ row normalized expression.
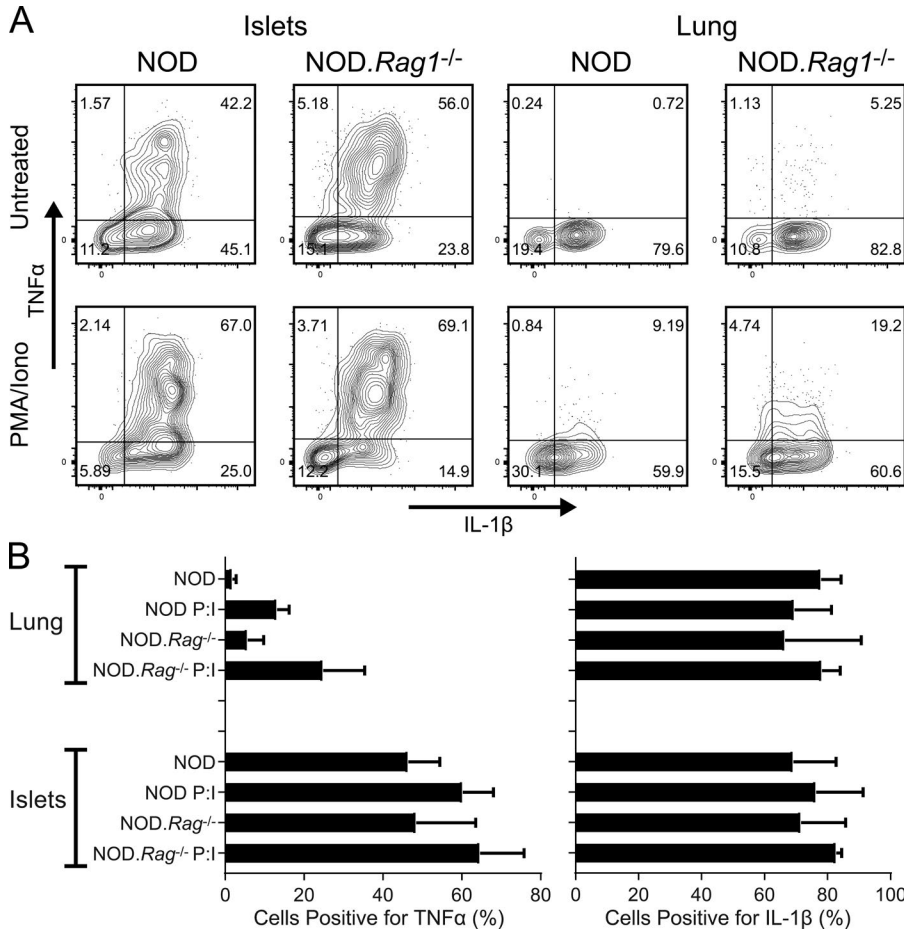
Figure 5. **Flow cytometric evaluation of islet macrophages for transcriptionally identified markers.** (A) The islets and lungs of 3-wk-old NOD and NOD.Rag1−/− mice were isolated and single-cell suspensions were made. Cells were stained with antibodies against cell surface markers and then fixed and stained with antibodies against intracellular pro-form IL-1β and TNF. Plots were gated on CD45+CD11c+MHC-II+CD11b+F4/80+. The percentages of cells positive are indicated in each quadrant. Results are representative of three independent experiments per condition. (B) Graphs of the percentage of macrophages positive for either TNF or IL-1β as determined in A. Bars show the mean ± SD for at least three independent experiments per condition.

al., 2011). In essence, the islet macrophages may be activated by intra–islet components as well as by blood products.

A second finding, as mentioned above, is the capacity of the islet macrophages to sense blood-borne stimuli. This finding opens the question of the biological significance of such sensing as well as on the repertoire of stimulants, an issue that needs critical evaluation. One needs to keep in mind that the $Tlr2^{−/−}$, $Tlr9^{−/−}$, and $Myd88^{−/−}$ mice have reduced incidences of diabetes (Kim et al., 2007; Wen et al., 2008; Tai et al., 2016). It is tempting to postulate that during weaning, profound changes occur in the islet macrophage, as was evident by MHC-II expression. This occurs at a time when the islet is subjected to more demands for growth as well as to a new intestinal flora. It is possible that the islet macrophage senses systemic inflammation, as suggested by the modulation of type 1 diabetes by gut flora and systemic infections (Wen et al., 2008; Christen and von Herrath, 2011; Markle et al., 2013; Yurkovetskiy et al., 2015). We speculate that through this sensory function, the macrophages play a protective role for the islets against blood-borne pathogens. Finally, one component that may contribute to NOD macrophage activation compared with NOD.Rag1−/− mice is the presence of antibodies, particularly those derived from the mother. Evidence in favor of this is that the wild-type heterozygote pups born from B

cell–deficient mice (μMT) display decreased incidence and penetrance of diabetes (Greeley et al., 2002).

The third finding is that there are genes characteristic of diabetes progression being expressed in 3-wk-old islet macrophages. This implies that even without overt lymphocyte infiltration of the islet or destruction of β cells, the adaptive immune system is enforcing a degree of activation on the islet macrophage. Thus, superimposed on the basal activation state, the diabetes susceptible traits impose a further activation program that is likely to be critical for the development and progression of the disease. The single-cell analysis of the islet-resident macrophages showed that only a subset of the NOD macrophages were more inflamed than those of the NOD.Rag1−/−. We cannot conclusively state which signal/cell type is responsible for the activation of the macrophage in a young NOD mouse, but the presence of an interferon signature points to an activated diabetogenic T cell acting on the islets at these early times. We have found a few T cells in islets at this early time period (Carrero et al., 2013). Also, up-regulation of the oxidative phosphorylation in NOD macrophages, as well as self-defense antioxidant enzyme expression (response to oxidative stress, GO term 0006979), suggests antimicrobial generation of ROS. Higher ROS synthesis in NOD macrophages compared with NOD.Rag1−/−
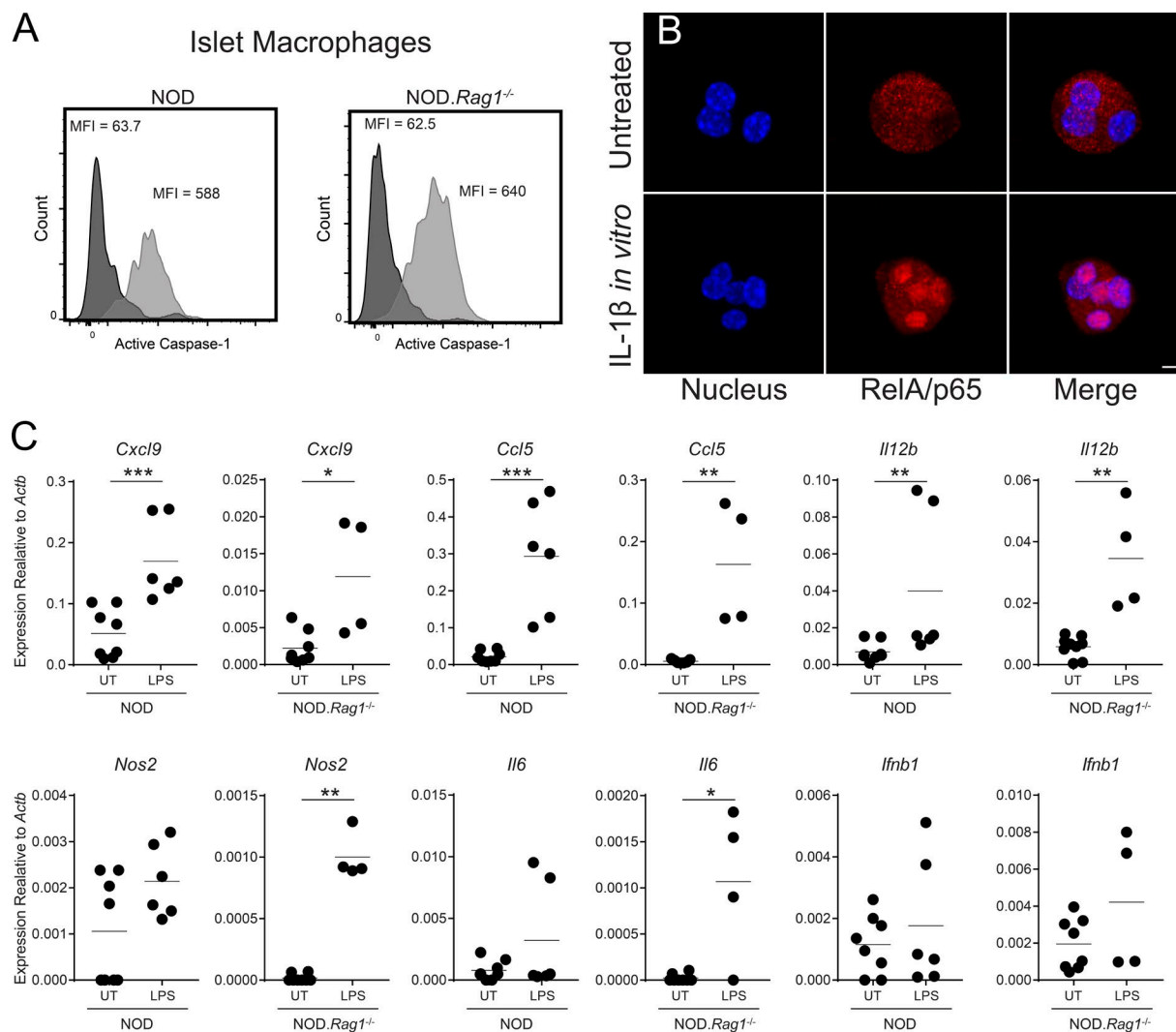
Figure 6. **Inflammatory status of islets before and after treatment with LPS.** (A) NOD or NOD.*Rag1*^{−/−} mouse islet macrophages were isolated and stained with the intracellular caspase-1 substrate FAM FLICA YVAD-FMK. The black histograms are gated on the CD45-negative fraction of the islets, and the gray histograms are gated on macrophages as in Fig. S1. Mean fluorescent intensity (MFI) is indicated on the graphs. MFIs for active caspase-1 ranged from 62.5–102 (mean 72.2) for the CD45^{neg} population and from 388–884 (mean 625) for the F4/80^{+} population. Data are representative of two or three independent experiments per group. (B) Islets from 6-wk-old NOD mice were isolated, dispersed, and cultured overnight in chamber slides in the absence or presence of IL-1β. Cells were then stained with DAPI (blue) and anti-RelA/p65 (red). Cells were imaged by confocal microscopy. Bar, 4 µm. Image is representative of three independent experiments. (C) Expression of inflammatory gene transcripts in macrophages isolated from islets of mice intravenously injected with LPS. The indicated mice were treated with either PBS (UT) or LPS IV (LPS). Then, islet macrophages were flow-sorted, RNA was isolated, and qRT-PCR was performed on the indicated markers. Each symbol represents one individually sorted sample. Horizontal bars show the mean. Significance was tested using the Mann-Whitney *U* test. *, P < 0.0332; **, P < 0.0021; ***, P < 0.0002. Graphs show all the data from at least three independent experiments performed in duplicate for each condition.

might be a result of synergistic action of adaptive and innate immune response (T cell and macrophage activation) as opposed to only an innate response in NOD.*Rag1*^{−/−}. During diabetogenesis, it is the lymphocytic infiltrate that is most likely responsible for the cell division and cellular activity signature in whole islets. Activated macrophages are known to express genes responsible not only for cytokine and chemokine production but also for cell cycle progression and proliferation (Buxadé et al., 2012).

Because NOD macrophage autoimmune activation is dependent on the presence of the adaptive immune system, it is likely that there is heterogeneity in immune components within a single islet or among them, with some affected and others not. Resolving this will require isolating single macrophages from individual hand-picked islets, a difficult task given current technologies. However, this will be an important issue to tackle, as it will instruct us as to the nature of the activation of the earliest sensors of autoimmune diabetes, the
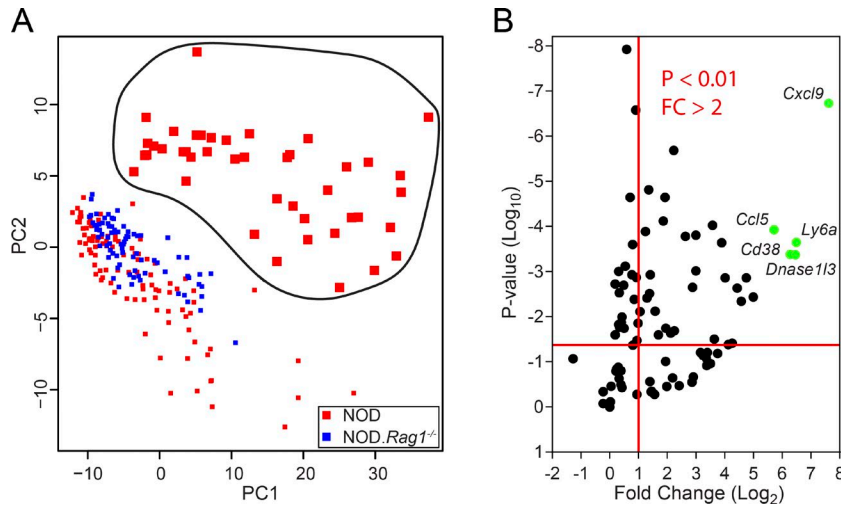
Figure 7. Single-cell qRT-PCR of islet macrophages reveals NOD heterogeneity. (A) PCA of the single-cell qRT-PCR results. The samples circled in black were all *Cxcl9*+, whereas no *Cxcl9*+ cells were found in the rest of the samples. PC, principal component. (B) Volcano plot of the fold change (FC; $\log_2$) expression between NOD and NOD.*Rag1*−/− compared with the ANOVA p-value ($\log_{10}$). Genes in the upper right quadrant had greater than twofold higher expression on average in NOD versus NOD.*Rag1*−/− and were significantly differentially expressed by ANOVA at $P < 0.01$.

macrophage, as well as the distribution of islet involvement in the autoimmune process. Thus, intervention and identification of those who will progress to diabetes must be done much earlier than diagnosis to intervene and prevent diabetes.

The islet macrophages express IL-1β and TNF at the steady state. Expression of IL-1β and TNF (and other cytokines) is a complex process (Aggarwal, 2003; Dinarello, 2009; Pasparakis, 2009). It involves several transcriptional regulators that modulate the level and time of expression of the gene (Foster et al., 2007; Amit et al., 2009; Yosef and Regev, 2011, 2016; Kotas and Medzhitov, 2015). This regulation is of particular relevance. As noted earlier, *Atf3* is expressed by the macrophages, indicating a degree of regulation of TLR signaling. Regarding IL-1β, we find an intermediate expression of active caspase-1 but failed to detect RelA by nuclear staining in the β cells. However, we may well be missing a low level of activation and are guarded in concluding a lack of IL-1β signaling in the β cell. Indeed, it is still likely that there is a level of homeostatic role for IL-1R signaling in endocrine function. For example, the p85α component of the PI3 kinase is activated by IL-1R signaling (Reddy et al., 1997). Deficiency of p85α leads to reduced insulin secretion after glucose challenge (Terauchi et al., 1999). Also, IL-1β treatment of islets instigates down-regulation of the glucose transporter GLUT2 and glucokinase (Park et al., 1999). Finally, IL-1R1-deficient mice develop late-onset obesity (García et al., 2006). In sum, IL-1 production by the islet macrophage may be one component in its general role as a modulator of glucose homeostasis influencing the pancreas, fat depots, and central nervous system (del Rey et al., 2006; Dror et al., 2017). Concerning its role in the autoimmune process, much has been discussed on IL-1's role in diabetes initiation, largely on the basis of the harmful effects of IL-1 on long-term cultures of β cells (Mandrup-Poulsen et al., 2010). However, a role in diabetes progression in the NOD mouse model is not evident. Genetic ablation of caspase-1 does not alter diabetes development (Schott et al., 2004).

IL-1R deficiency delays progression to diabetes, albeit modestly (Thomas et al., 2004). As for TNF, its effects are pleiotropic but are also under strict control. TNF can affect not only β cells but also the vascular endothelium and T cells. In contrast to IL-1β, TNF has complex effects on diabetes development, most likely on the effector stage of the disease by modifying not only β cells but also T cells (Yang et al., 1994; Kägi et al., 1999; Pakala et al., 1999; Wu et al., 2002; Chee et al., 2011).

The data indicate that the islet macrophage is subjected to stimuli derived from β cells as well as by blood products (Calderon et al., 2011; Vomund et al., 2015). Therefore, this leads to a transcriptional program that is complex, representing the diverse stimuli, and these responses need to be integrated. In the absence of macrophages as in the *op/op* mouse the development of islets is impaired (Banaei-Bouchareb et al., 2004). Studies are now under way in our laboratory to determine the activation state of islet macrophages derived from different strains and ages of mice and under different biological conditions. The islet macrophages of all strains examined contain macrophages with core features similar to NOD.*Rag1*−/−. In contrast, the signature of diabetic inflammation that includes *Cxcl9* and other interferon-inducible genes has been found only in NOD, not in any of the control strains.

MATERIALS AND METHODS
Mice
NOD/ShiLtJ (NOD), NOD.129S7(B6)-*Rag1*tm1Mom/J (NOD.*Rag1*−/−), and B6.NOD-(D17Mit21-D17Mit10)/LtJ (B6.g7) mice originally obtained from The Jackson Laboratory were bred and maintained under specific pathogen-free conditions in our animal facility. All experiments were approved by the Division of Comparative Medicine of Washington University School of Medicine in St. Louis (Association for Assessment and Accreditation of Laboratory Animal Care, accreditation number A3381-01).

Antibodies

The following antibodies were purchased from BioLegend: FITC/PE/PerCP-Cy5.5 anti-B220 (RA3-6B2), PE-Cy7 anti-CD11b (M1/70), PE/APC-Cy7 anti-CD11c (N418), PE/APC anti-CD274 (10F.9G2), PE-Cy7 anti-CD4 (RM4-5), APC-Cy7 anti-CD44 (IM7), BV510/APC anti-CD45 (30-F11), FITC anti-CD53 (OX-79), FITC/PerCP-Cy5.5 anti-CD8a (53-6.7), PE-Cy7 anti-CD83 (Michel-19), FITC/APC anti-F4/80 (BM8), and APC anti-TNF (MP6-XT22). The following antibodies were purchased from eBioscience: fixable viability dye eflour780 and PerCP eflour710 proIL-1β (NJTEN3). The following antibodies were purchased from BD: FITC/APC anti-CD3e (145-2C11), PE anti-IFNγ (XMG1.2), and PE anti-TLR7 (A94B10). Pacific Blue I-A^{g7} (AG2.42.7) was made in our laboratory (Suri et al., 2002).

Flow cytometry and cell sorting

Islets were harvested as described previously (Calderon et al., 2015) and dispersed using Cell Dissociation Solution Non-Enzymatic (Sigma-Aldrich) for 5 min at 37°C. PLNs and lungs were harvested, finely chopped with scissors, placed in DMEM (Thermo Fisher Scientific) containing 125 μg/ml Liberase TL (Roche) and 50 μg/ml DNase I, grade II (Roche), and incubated at 37°C for 30 min and dispersed via gentle agitation. Single-cell suspensions incubated in PBS, pH 7.4 (Thermo Fisher Scientific) having 1% BSA (Sigma-Aldrich), and 50% of 2.4G2 conditioned DMEM at 4°C for 15 min to block Fc receptors. Cells were stained with fluorescently labeled antibodies and sorted using a FACSAria II or analyzed using the FACSCanto II (BD). Macrophages were sorted on the basis of their expression of CD45, F4/80, and I-A^{g7}. DCs were selected on the basis of their expression of XCR1. In all cases CD3e$^+$ and CD19$^+$ events were eliminated from the sort (dump gated). For cell sorting experiments, ~500–5,000 macrophages were isolated from 6–10 mice, and this represented 1 biological sample in our analysis. At least three samples were used for each population studied by RNASeq analysis. All flow cytometry data were analyzed using FlowJo software version 10.2 (Tree Star).

Intravenous LPS injection

NOD and NOD.Rag1$^{-/-}$ mice were intravenously injected with 100 ng LPS in 0.1 ml PBS. Mouse islets were harvested 3 h later and dispersed, and macrophages were sorted using the FACSAria II (BD) after staining with antibodies to CD45, CD3, CD19, F4/80, and I-A^{g7}.

RNA isolation and real-time PCR

Sorted cell RNA was isolated using the Ambion RNAqueous-Micro kit (Thermo Fisher Scientific) following the manufacturer's instructions. RNA was quantified by OD260 using NanoDrop (Thermo Fisher Scientific). cDNA was synthesized using iScript Reverse Transcription Supermix for qRT-PCR (Bio-Rad Laboratories). qRT-PCR was performed using the 5′ nuclease (TaqMan) chemistry using iTaq Universal Probes Supermix (Bio-Rad Laboratories). The 18S ribosomal RNA probe was obtained from Thermo Fisher Scientific, and all other primers and probes were designed and obtained from IDT DNA. All quantitative PCRs were performed on a StepOnePlus Real-Time PCR system (Thermo Fisher Scientific) running StepOne 2.3 Software (Thermo Fisher Scientific). Quality control was performed by the StepOne 2.3 software. RT-PCR data analysis was done using Excel (Microsoft).

RNASeq analysis

Library preparation was performed with 1–50 ng total RNA; integrity was determined using an Agilent Bioanalyzer (Agilent Technologies). Double-stranded cDNA was prepared using the SeqPlex RNA Amplification kit (Sigma-Aldrich) per the manufacturer's protocol. cDNA was blunt ended, had an adenosine added to the 3′ ends, and then had Illumina sequencing adapters ligated to the ends. Ligated fragments were then amplified for 12 cycles using primers incorporating unique index tags. Fragments were sequenced on an Illumina HiSeq-2500 using single reads extending 50 bases. All RNASeq work was performed by the Genome Technology Access Center at Washington University School of Medicine.

We assessed the mean quality of sequencing reads for base pair positions in each sample using the fastqc utility from fastq-tools (Droop, 2016). Samples with a quality score less than 25 (Sanger/Illumina 1.9 encoding) across all bases were truncated using the fastx_trimmer utility, removing base pairs from the end of each read in the library. All libraries were aligned to the GRCm38.p4 assembly of the mouse genome using the STAR aligner (Dobin et al., 2013) with GEN CODE version M7 (Harrow et al., 2012) transcripts included into the pregenerated reference. We generated raw counts of the number of tags on each gene by using htseq-count utility from the HTseq package (Anders et al., 2015). GENCODE version M7 (with -t exon option) was used as a reference GTF. The DESeq2 package (version 1.6.3; Love et al., 2014) was used to detect differentially expressed genes between the analyzed conditions (output with P < 0.05 and a Benjamini-Hochberg FDR of 5% was used). Variance between samples was stabilized for the purposes of hierarchical clustering and PCA to address the problem of heteroscedasticity (dependence of variance on the mean counts). Pathways analysis was done using the Broad Institute's GSEA software (Subramanian et al., 2005). All heat maps are in log$_2$ scale.

LPS, TNF, and IL–1 signature analysis

The LPS signature consists of genes up-regulated in macrophages treated with LPS for 40 min when compared with untreated macrophages at P < 0.05, log fold change >1 (GSE14769). The IL-1 signature consists of genes up-regulated in human monocyte-derived macrophages 4 h after stimulation with IL-1 compared with control cells (GSE8515, P < 0.05, log fold change >0.7). The donor effect for the GSE8515 data set was corrected with ComBat (Johnson et

al., 2007). The limma package was used for differential expression analysis of microarray data (Ritchie et al., 2015). The TNF signaling gene set was taken from the Broad Institute Molecular Signatures Database (MSigDB) hallmark gene sets (Hallmark TNF signaling via NF-κB). The ImmGen dataset was downloaded from GEO (GSE15907; Heng et al., 2008).

Intracellular flow cytometry

Dispersed islet or PLN cells were placed at 37°C in DMEM, 10% FBS (GE Healthcare), and 10 µg/ml Brefeldin A for 4 h. As a positive control for activation, samples were pulsed with 100 ng/ml PMA (Sigma-Aldrich) and 500 ng/ml ionomycin (Sigma-Aldrich). Cells were washed with PBS, 1% BSA, cell surface stained with fluorescent antibodies for 30 min at 4°C, and fixed with PBS and 2% formaldehyde (Sigma-Aldrich) for 15 min at 4°C. Cells were washed with PBS and 1% BSA, incubated with 2% saponin (Sigma-Aldrich) and PBS for 5 min at 4°C, and then with fluorescent antibodies recognizing intracellular proteins for 30 min at 4°C. Cells were washed with 2% saponin and PBS and then with PBS and 1% BSA. Flow cytometry was performed using a FACSCanto II.

Immunofluorescence microscopy

For nuclear RelA detection, islets from 6-wk-old NOD females were isolated and dispersed as described previously. Dispersed cells were placed in chamber slides and incubated at 37°C overnight in 20 ng/ml IL-1β (PeproTech) DMEM (Thermo Fisher Scientific) supplemented with 10% FGE (Healthcare Life Sciences) or in DMEM 10% FBS alone (Rütti et al., 2016). Cells were washed with 1% BSA in PBS and fixed and permeabilized using the BD Fix/Perm kit according to the manufacturer's instructions. Cells were stained with NF-κB p65 (D14E12) XP rabbit mAb (Cell Signaling Technology) overnight at 4°C. Cells were washed twice with PBS and stained with Alexa 488 anti-rabbit IgG F(ab')^2 (Cell Signaling Technology) for 2 h at room temperature. After washing with PBS, the chamber was removed, and Prolong Gold Anti-Fade Reagent with DAPI (Cell Signaling Technology) was applied. Slides were imaged using a Leica SPE confocal microscope.

For pancreas immunofluorescence, frozen sections from each tissue were cut on a cryotome at 10 µm. Sections were fixed for 5 min in ice-cold acetone. Then the sections were blocked with Cas-Block (Thermo Fisher Scientific) following the manufacturer's instructions. The sections were then stained with PE anti-B220 (RA3-6B2), PE anti-Siglec H (551), or PE anti-Ly6G (1A8; eBioscience) and polyclonal guinea pig anti-insulin (Thermo Fisher Scientific) for 1 h at room temperature. Sections were washed three times with PBS and then stained with goat anti–guinea pig Alexa-488 (A11073; Thermo Fisher Scientific) for 1 h at room temperature. Background autofluorescence was quenched with 70% ethanol supplemented with 0.5% Sudan Black B (Sigma-Aldrich) for 2 min at room temperature and washed with PBS. Nuclei were stained with bisBenzimide H 33258 (Sigma-

Aldrich) at a concentration of 1 µg/ml in water for 5 min at room temperature and washed three times with PBS. Sections were mounted with PBS containing 50% glycerol and visualized via an Olympus BX51 microscope.

Active caspase–1 detection

Islets were isolated and dispersed as described previously. Cells were incubated for 30 min at 37°C with the fluorescent inhibitor probe FAM-YVAD-FMK (Immunochemistry Technologies) to label active caspase-1 enzyme. Cells were washed and stained for cell surface antigens, acquired using a FACSCanto II flow cytometer, and analyzed using FlowJo software.

Single–cell sorting and quantitative PCR

Islet macrophages were isolated, stained, and single-cell-sorted into 96-well plates containing 5 µl Cellsdirect 2X Reaction Mix (Thermo Fisher Scientific) and 0.1 µl RNase inhibitor (SUPERase-In; Thermo Fisher Scientific) per well. For reverse transcription and specific cDNA preamplification, all the 96 20× Taqman assays (Fig. S5; IDT DNA) were mixed and diluted to 0.2×. Subsequently, 2.5 µl of the 0.2× Taqman assay mix, 0.2 µl of the SuperScript III RT/Platinum Taq (Thermo Fisher Scientific), and 1.2 µl PCR-certified water (Thermo Fisher Scientific) were added together to the sorted single cells. Reverse transcription (15 min at 50°C) was performed, followed by Taq activation (2 min at 95°C) and 18 cycles of cDNA preamplification (each cycle: 15 s at 95°C, 4 min at 60°C). The resulting cDNA product was diluted with PCR-certified water (1:5) and submitted for single-cell quantitative PCR using the Biomark HD system (Fluidigm).

Data availability

RNAseq data are available at the Gene Expression Omnibus under accession no. GSE100067.

Online supplemental material

Fig. S1 shows the gating strategy for the isolated cells, expression of MHC on macrophages from ImmGen, and flow cytometry of cell surface markers on islet macrophages. Fig. S2 shows immunofluorescence of pancreas and lymphoid structures. Fig. S3 shows different islet isolation techniques and outcomes. Fig. S4 shows Pearson correlation, heat maps, and gene set enrichment analysis. Fig. S5 shows single-cell islet macrophage qRT-PCR data. Table S1, included in a separate Excel file, shows the normalized gene counts for the dataset.

REFERENCES

Aggarwal, B.B. 2003. Signalling pathways of the TNF superfamily: a double-edged sword. *Nat. Rev. Immunol.* 3:745–756. http://dx.doi.org/10.1038/nri1184

Amit, I., M. Garber, N. Chevrier, A.P. Leite, Y. Donner, T. Eisenhaure, M. Guttman, J.K. Grenier, W. Li, O. Zuk, et al. 2009. Unbiased reconstruction of a mammalian transcriptional network mediating pathogen responses. *Science.* 326:257–263. http://dx.doi.org/10.1126/science.1179050

Amit, I., D.R. Winter, and S. Jung. 2016. The role of the local environment and epigenetics in shaping macrophage identity and their effect on tissue homeostasis. *Nat. Immunol.* 17:18–25. http://dx.doi.org/10.1038/ni.3325

Anders, S., P.T. Pyl, and W. Huber. 2015. HTSeq—a Python framework to work with high-throughput sequencing data. *Bioinformatics.* 31:166–169. http://dx.doi.org/10.1093/bioinformatics/btu638

Andrade, W.A., A.M. Silva, V.S. Alves, A.P. Salgado, M.B. Melo, H.M. Andrade, F.V. Dall'Orto, S.A. Garcia, T.N. Silveira, and R.T. Gazzinelli. 2010. Early endosome localization and activity of RasGEF1b, a toll-like receptor-inducible Ras guanine-nucleotide exchange factor. *Genes Immun.* 11:447–457. http://dx.doi.org/10.1038/gene.2009.107

Banaei-Bouchareb, L., V. Gouon-Evans, D. Samara-Boustani, M.C. Castellotti, P. Czernichow, J.W. Pollard, and M. Polak. 2004. Insulin cell mass is altered in Csf1op/Csf1op macrophage-deficient mice. *J. Leukoc. Biol.* 76:359–367. http://dx.doi.org/10.1189/jlb.1103591

Buxadé, M., G. Lunazzi, J. Minguillón, S. Iborra, R. Berga-Bolaños, M. Del Val, J. Aramburu, and C. López-Rodríguez. 2012. Gene expression induced by Toll-like receptors in macrophages requires the transcription factor NFAT5. *J. Exp. Med.* 209:379–393. http://dx.doi.org/10.1084/jem.20111569

Calderon, B., A. Suri, M.J. Miller, and E.R. Unanue. 2008. Dendritic cells in islets of Langerhans constitutively present beta cell-derived peptides bound to their class II MHC molecules. *Proc. Natl. Acad. Sci. USA.* 105:6121–6126. http://dx.doi.org/10.1073/pnas.0801973105

Calderon, B., J.A. Carrero, M.J. Miller, and E.R. Unanue. 2011. Cellular and molecular events in the localization of diabetogenic T cells to islets of Langerhans. *Proc. Natl. Acad. Sci. USA.* 108:1561–1566. http://dx.doi.org/10.1073/pnas.1018973108

Calderon, B., J.A. Carrero, S.T. Ferris, D.K. Sojka, L. Moore, S. Epelman, K.M. Murphy, W.M. Yokoyama, G.J. Randolph, and E.R. Unanue. 2015. The pancreas anatomy conditions the origin and properties of resident macrophages. *J. Exp. Med.* 212:1497–1512. http://dx.doi.org/10.1084/jem.20150496

Carrero, J.A., B. Calderon, F. Towfic, M.N. Artyomov, and E.R. Unanue. 2013. Defining the transcriptional and cellular landscape of type 1 diabetes in the NOD mouse. *PLoS One.* 8:e59701. http://dx.doi.org/10.1371/journal.pone.0059701

Castellino, F., A.Y. Huang, G. Altan-Bonnet, S. Stoll, C. Scheinecker, and R.N. Germain. 2006. Chemokines enhance immunity by guiding naive CD8+ T cells to sites of CD4+ T cell-dendritic cell interaction. *Nature.* 440:890–895. http://dx.doi.org/10.1038/nature04651

Chee, J., E. Angstetra, L. Mariana, K.L. Graham, E.M. Carrington, H. Bluethmann, P. Santamaria, J. Allison, T.W.H. Kay, B. Krishnamurthy, and H.E. Thomas. 2011. TNF receptor 1 deficiency increases regulatory T cell function in nonobese diabetic mice. *J. Immunol.* 187:1702–1712. http://dx.doi.org/10.4049/jimmunol.1100511

Chen, L., and D.B. Flies. 2013. Molecular mechanisms of T cell co-stimulation and co-inhibition. *Nat. Rev. Immunol.* 13:227–242. http://dx.doi.org/10.1038/nri3405

Chevrier, N., P. Mertins, M.N. Artyomov, A.K. Shalek, M. Iannacone, M.F. Ciaccio, I. Gat-Viks, E. Tonti, M.M. DeGrace, K.R. Clauser, et al. 2011. Systematic discovery of TLR signaling components delineates viral-sensing circuits. *Cell.* 147:853–867. http://dx.doi.org/10.1016/j.cell.2011.10.022

Christen, U., and M.G. von Herrath. 2011. Do viral infections protect from or enhance type 1 diabetes and how can we tell the difference? *Cell. Mol. Immunol.* 8:193–198. http://dx.doi.org/10.1038/cmi.2010.71

del Rey, A., E. Roggero, A. Randolf, C. Mahuad, S. McCann, V. Rettori, and H.O. Besedovsky. 2006. IL-1 resets glucose homeostasis at central levels. *Proc. Natl. Acad. Sci. USA.* 103:16039–16044. http://dx.doi.org/10.1073/pnas.0607076103

Diana, J., and A. Lehuen. 2014. Macrophages and β-cells are responsible for CXCR2-mediated neutrophil infiltration of the pancreas during autoimmune diabetes. *EMBO Mol. Med.* 6:1090–1104. http://dx.doi.org/10.15252/emmm.201404144

Diana, J., Y. Simoni, L. Furio, L. Beaudoin, B. Agerberth, F. Barrat, and A. Lehuen. 2013. Crosstalk between neutrophils, B-1a cells and plasmacytoid dendritic cells initiates autoimmune diabetes. *Nat. Med.* 19:65–73. http://dx.doi.org/10.1038/nm.3042

Dinarello, C.A. 2009. Immunological and inflammatory functions of the interleukin-1 family. *Annu. Rev. Immunol.* 27:519–550. http://dx.doi.org/10.1146/annurev.immunol.021908.132612

Dobin, A., C.A. Davis, F. Schlesinger, J. Drenkow, C. Zaleski, S. Jha, P. Batut, M. Chaisson, and T.R. Gingeras. 2013. STAR: ultrafast universal RNA-seq aligner. *Bioinformatics.* 29:15–21. http://dx.doi.org/10.1093/bioinformatics/bts635

Droop, A.P. 2016. fqtools: an efficient software suite for modern FASTQ file manipulation. *Bioinformatics.* 32:1883–1884. http://dx.doi.org/10.1093/bioinformatics/btw088

Dror, E., E. Dalmas, D.T. Meier, S. Wueest, J. Thévenet, C. Thienel, K. Timper, T.M. Nordmann, S. Traub, F. Schulze, et al. 2017. Postprandial macrophage-derived IL-1β stimulates insulin, and both synergistically promote glucose disposal and inflammation. *Nat. Immunol.* 18:283–292. http://dx.doi.org/10.1038/ni.3659

Dufour, J.H., M. Dziejman, M.T. Liu, J.H. Leung, T.E. Lane, and A.D. Luster. 2002. IFN-gamma-inducible protein 10 (IP-10; CXCL10)-deficient mice reveal a role for IP-10 in effector T cell generation and trafficking. *J. Immunol.* 168:3195–3204. http://dx.doi.org/10.4049/jimmunol.168.7.3195

Ewald, S.E., A. Engel, J. Lee, M. Wang, M. Bogyo, and G.M. Barton. 2011. Nucleic acid recognition by Toll-like receptors is coupled to stepwise processing by cathepsins and asparagine endopeptidase. *J. Exp. Med.* 208:643–651. http://dx.doi.org/10.1084/jem.20100682

Ferris, S.T., J.A. Carrero, J.F. Mohan, B. Calderon, K.M. Murphy, and E.R. Unanue. 2014. A minor subset of Batf3-dependent antigen-presenting cells in islets of Langerhans is essential for the development of autoimmune diabetes. *Immunity.* 41:657–669. http://dx.doi.org/10.1016/j.immuni.2014.09.012

Foster, S.L., D.C. Hargreaves, and R. Medzhitov. 2007. Gene-specific control of inflammation by TLR-induced chromatin modifications. *Nature.* 447:972–978.

Fridovich, I. 1995. Superoxide radical and superoxide dismutases. *Annu. Rev. Biochem.* 64:97–112. http://dx.doi.org/10.1146/annurev.bi.64.070195.000525

García, M.C., I. Wernstedt, A. Berndtsson, M. Enge, M. Bell, O. Hultgren, M. Horn, B. Ahrén, S. Enerback, C. Ohlsson, et al. 2006. Mature-onset obesity in interleukin-1 receptor I knockout mice. *Diabetes.* 55:1205–1213. http://dx.doi.org/10.2337/db05-1304

Gautier, E.L., T. Shay, J. Miller, M. Greter, C. Jakubzick, S. Ivanov, J. Helft, A. Chow, K.G. Elpek, S. Gordonov, et al. Immunological Genome Consortium. 2012. Gene-expression profiles and transcriptional regulatory pathways that underlie the identity and diversity of mouse tissue macrophages. *Nat. Immunol.* 13:1118–1128. http://dx.doi.org/10.1038/ni.2419

Gilchrist, M., V. Thorsson, B. Li, A.G. Rust, M. Korb, J.C. Roach, K. Kennedy, T. Hai, H. Bolouri, and A. Aderem. 2006. Systems biology approaches identify ATF3 as a negative regulator of Toll-like receptor 4. *Nature.* 441:173–178. http://dx.doi.org/10.1038/nature04768

Greeley, S.A.W., M. Katsumata, L. Yu, G.S. Eisenbarth, D.J. Moore, H. Goodarzi, C.F. Barker, A. Naji, and H. Noorchashm. 2002. Elimination of maternally transmitted autoantibodies prevents diabetes in nonobese diabetic mice. *Nat. Med.* 8:399–402. http://dx.doi.org/10.1038/nm0402-399

Griffith, J.W., C.L. Sokol, and A.D. Luster. 2014. Chemokines and chemokine receptors: positioning cells for host defense and immunity. *Annu. Rev. Immunol.* 32:659–702. http://dx.doi.org/10.1146/annurev-immunol-032713-120145

Haldar, M., M. Kohyama, A.Y. So, W. Kc, X. Wu, C.G. Briseño, A.T. Satpathy, N.M. Kretzer, H. Arase, N.S. Rajasekaran, et al. 2014. Heme-mediated SPI-C induction promotes monocyte differentiation into iron-recycling macrophages. *Cell.* 156:1223–1234. http://dx.doi.org/10.1016/j.cell.2014.01.069

Harrow, J., A. Frankish, J.M. Gonzalez, E. Tapanari, M. Diekhans, F. Kokocinski, B.L. Aken, D. Barrell, A. Zadissa, S. Searle, et al. 2012. GENCODE: the reference human genome annotation for the ENCODE Project. *Genome Res.* 22:1760–1774. http://dx.doi.org/10.1101/gr.135350.111

Heng, T.S., and M.W. Painter. Immunological Genome Project Consortium. 2008. The Immunological Genome Project: networks of gene expression in immune cells. *Nat. Immunol.* 9:1091–1094. http://dx.doi.org/10.1038/ni1008-1091

Johnson, W.E., C. Li, and A. Rabinovic. 2007. Adjusting batch effects in microarray expression data using empirical Bayes methods. *Biostatistics.* 8:118–127. http://dx.doi.org/10.1093/biostatistics/kxj037

Kägi, D., A. Ho, B. Odermatt, A. Zakarian, P.S. Ohashi, and T.W. Mak. 1999. TNF receptor 1-dependent beta cell toxicity as an effector pathway in autoimmune diabetes. *J. Immunol.* 162:4598–4605.

Kaikkonen, M.U., N.J. Spann, S. Heinz, C.E. Romanoski, K.A. Allison, J.D. Stender, H.B. Chun, D.F. Tough, R.K. Prinjha, C. Benner, and C.K. Glass. 2013. Remodeling of the enhancer landscape during macrophage activation is coupled to enhancer transcription. *Mol. Cell.* 51:310–325. http://dx.doi.org/10.1016/j.molcel.2013.07.010

Kanehisa, M., and S. Goto. 2000. KEGG: kyoto encyclopedia of genes and genomes. *Nucleic Acids Res.* 28:27–30. http://dx.doi.org/10.1093/nar/28.1.27

Kawai, T., and S. Akira. 2011. Toll-like receptors and their crosstalk with other innate receptors in infection and immunity. *Immunity.* 34:637–650. http://dx.doi.org/10.1016/j.immuni.2011.05.006

Kim, H.S., M.S. Han, K.W. Chung, S. Kim, E. Kim, M.J. Kim, E. Jang, H.A. Lee, J. Youn, S. Akira, and M.S. Lee. 2007. Toll-like receptor 2 senses beta-cell death and contributes to the initiation of autoimmune diabetes. *Immunity.* 27:321–333. http://dx.doi.org/10.1016/j.immuni.2007.06.010

Koblansky, A.A., D. Jankovic, H. Oh, S. Hieny, W. Sungnak, R. Mathur, M.S. Hayden, S. Akira, A. Sher, and S. Ghosh. 2013. Recognition of profilin by Toll-like receptor 12 is critical for host resistance to Toxoplasma gondii. *Immunity.* 38:119–130. http://dx.doi.org/10.1016/j.immuni.2012.09.016

Kotas, M.E., and R. Medzhitov. 2015. Homeostasis, inflammation, and disease susceptibility. *Cell.* 160:816–827. http://dx.doi.org/10.1016/j.cell.2015.02.010

Kurth, I., K. Willimann, P. Schaerli, T. Hunziker, I. Clark-Lewis, and B. Moser. 2001. Monocyte selectivity and tissue localization suggests a role for breast and kidney-expressed chemokine (BRAK) in macrophage development. *J. Exp. Med.* 194:855–862. http://dx.doi.org/10.1084/jem.194.6.855

Lavin, Y., D. Winter, R. Blecher-Gonen, E. David, H. Keren-Shaul, M. Merad, S. Jung, and I. Amit. 2014. Tissue-resident macrophage enhancer landscapes are shaped by the local microenvironment. *Cell.* 159:1312–1326. http://dx.doi.org/10.1016/j.cell.2014.11.018

Litvak, V., S.A. Ramsey, A.G. Rust, D.E. Zak, K.A. Kennedy, A.E. Lampano, M. Nykter, I. Shmulevich, and A. Aderem. 2009. Function of C/EBPdelta in a regulatory circuit that discriminates between transient and persistent TLR4-induced signals. *Nat. Immunol.* 10:437–443. http://dx.doi.org/10.1038/ni.1721

Love, M.I., W. Huber, and S. Anders. 2014. Moderated estimation of fold change and dispersion for RNA-seq data with DESeq2. *Genome Biol.* 15:550. http://dx.doi.org/10.1186/s13059-014-0550-8

Mandrup-Poulsen, T., L. Pickersgill, and M.Y. Donath. 2010. Blockade of interleukin 1 in type 1 diabetes mellitus. *Nat. Rev. Endocrinol.* 6:158–166. http://dx.doi.org/10.1038/nrendo.2009.271

Markle, J.G.M., D.N. Frank, S. Mortin-Toth, C.E. Robertson, L.M. Feazel, U. Rolle-Kampczyk, M. von Bergen, K.D. McCoy, A.J. Macpherson, and J.S. Danska. 2013. Sex differences in the gut microbiome drive hormone-dependent regulation of autoimmunity. *Science.* 339:1084–1088. http://dx.doi.org/10.1126/science.1233521

Matloubian, M., A. David, S. Engel, J.E. Ryan, and J.G. Cyster. 2000. A transmembrane CXC chemokine is a ligand for HIV-coreceptor Bonzo. *Nat. Immunol.* 1:298–304. http://dx.doi.org/10.1038/79738

Melli, K., R.S. Friedman, A.E. Martin, E.B. Finger, G. Miao, G.L. Szot, M.F. Krummel, and Q. Tang. 2009. Amplification of autoimmune response through induction of dendritic cell maturation in inflamed tissues. *J. Immunol.* 182:2590–2600. http://dx.doi.org/10.4049/jimmunol.0803543

Mi, H., A. Muruganujan, J.T. Casagrande, and P.D. Thomas. 2013. Large-scale gene function analysis with the PANTHER classification system. *Nat. Protoc.* 8:1551–1566. http://dx.doi.org/10.1038/nprot.2013.092

Mi, H., S. Poudel, A. Muruganujan, J.T. Casagrande, and P.D. Thomas. 2016. PANTHER version 10: expanded protein families and functions, and analysis tools. *Nucleic Acids Res.* 44(D1):D336–D342. http://dx.doi.org/10.1093/nar/gkv1194

Miller, J.C., B.D. Brown, T. Shay, E.L. Gautier, V. Jojic, A. Cohain, G. Pandey, M. Leboeuf, K.G. Elpek, J. Helft, et al. Immunological Genome Consortium. 2012. Deciphering the transcriptional network of the dendritic cell lineage. *Nat. Immunol.* 13:888–899. http://dx.doi.org/10.1038/ni.2370

Mootha, V.K., C.M. Lindgren, K.-F. Eriksson, A. Subramanian, S. Sihag, J. Lehar, P. Puigserver, E. Carlsson, M. Ridderstråle, E. Laurila, et al. 2003. PGC-1α-responsive genes involved in oxidative phosphorylation are

coordinately downregulated in human diabetes. *Nat. Genet.* 34:267–273. http://dx.doi.org/10.1038/ng1180

Moratz, C., J.R. Hayman, H. Gu, and J.H. Kehrl. 2004. Abnormal B-cell responses to chemokines, disturbed plasma cell localization, and distorted immune tissue architecture in Rgs1$^{-/-}$ mice. *Mol. Cell. Biol.* 24:5767–5775. http://dx.doi.org/10.1128/MCB.24.13.5767-5775.2004

Oldenburg, M., A. Krüger, R. Ferstl, A. Kaufmann, G. Nees, A. Sigmund, B. Bathke, H. Lauterbach, M. Suter, S. Dreher, et al. 2012. TLR13 recognizes bacterial 23S rRNA devoid of erythromycin resistance–forming modification. *Science.* 337:1111–1115. http://dx.doi.org/10.1126/science.1220363

Pakala, S.V., M. Chivetta, C.B. Kelly, and J.D. Katz. 1999. In autoimmune diabetes the transition from benign to pernicious insulitis requires an islet cell response to tumor necrosis factor alpha. *J. Exp. Med.* 189:1053–1062. http://dx.doi.org/10.1084/jem.189.7.1053

Park, C., J.R. Kim, J.K. Shim, B.S. Kang, Y.G. Park, K.S. Nam, Y.C. Lee, and C.H. Kim. 1999. Inhibitory effects of streptozotocin, tumor necrosis factor–alpha, and interleukin-1beta on glucokinase activity in pancreatic islets and gene expression of GLUT2 and glucokinase. *Arch. Biochem. Biophys.* 362:217–224. http://dx.doi.org/10.1006/abbi.1998.1004

Pasparakis, M. 2009. Regulation of tissue homeostasis by NF-kappaB signalling: implications for inflammatory diseases. *Nat. Rev. Immunol.* 9:778–788. http://dx.doi.org/10.1038/nri2655

Reddy, S.A.G., J.H. Huang, and W.S.-L. Liao. 1997. Phosphatidylinositol 3-kinase in interleukin 1 signaling. Physical interaction with the interleukin 1 receptor and requirement in NFκB and AP-1 activation. *J. Biol. Chem.* 272:29167–29173. http://dx.doi.org/10.1074/jbc.272.46.29167

Reif, K., and J.G. Cyster. 2000. RGS molecule expression in murine B lymphocytes and ability to down-regulate chemotaxis to lymphoid chemokines. *J. Immunol.* 164:4720–4729. http://dx.doi.org/10.4049/jimmunol.164.9.4720

Ritchie, M.E., B. Phipson, D. Wu, Y. Hu, C.W. Law, W. Shi, and G.K. Smyth. 2015. limma powers differential expression analyses for RNA-sequencing and microarray studies. *Nucleic Acids Res.* 43:e47. http://dx.doi.org/10.1093/nar/gkv007

Rütti, S., C. Howald, C. Arous, E. Dermitzakis, P.A. Halban, and K. Bouzakri. 2016. IL-13 improves beta-cell survival and protects against IL-1beta-induced beta-cell death. *Mol. Metab.* 5:122–131. http://dx.doi.org/10.1016/j.molmet.2015.11.003

Schott, W.H., B.D. Haskell, H.M. Tse, M.J. Milton, J.D. Piganelli, C.M. Choisy-Rossi, P.C. Reifsnyder, A.V. Chervonsky, and E.H. Leiter. 2004. Caspase-1 is not required for type 1 diabetes in the NOD mouse. *Diabetes.* 53:99–104. http://dx.doi.org/10.2337/diabetes.53.1.99

Smyth, D.J., V. Plagnol, N.M. Walker, J.D. Cooper, K. Downes, J.H.M. Yang, J.M.M. Howson, H. Stevens, R. McManus, C. Wijmenga, et al. 2008. Shared and distinct genetic variants in type 1 diabetes and celiac disease. *N. Engl. J. Med.* 359:2767–2777. http://dx.doi.org/10.1056/NEJMoa0807917

Subramanian, A., P. Tamayo, V.K. Mootha, S. Mukherjee, B.L. Ebert, M.A. Gillette, A. Paulovich, S.L. Pomeroy, T.R. Golub, E.S. Lander, and J.P. Mesirov. 2005. Gene set enrichment analysis: a knowledge-based approach for interpreting genome-wide expression profiles. *Proc. Natl. Acad. Sci. USA.* 102:15545–15550. http://dx.doi.org/10.1073/pnas.0506580102

Suri, A., I. Vidavsky, K. van der Drift, O. Kanagawa, M.L. Gross, and E.R. Unanue. 2002. In APCs, the autologous peptides selected by the diabetogenic I-Ag7 molecule are unique and determined by the amino acid changes in the P9 pocket. *J. Immunol.* 168:1235–1243. http://dx.doi.org/10.4049/jimmunol.168.3.1235

Tai, N., F.S. Wong, and L. Wen. 2016. The role of the innate immune system in destruction of pancreatic beta cells in NOD mice and humans with type I diabetes. *J. Autoimmun.* 71:26–34. http://dx.doi.org/10.1016/j.jaut.2016.03.006

Terauchi, Y., Y. Tsuji, S. Satoh, H. Minoura, K. Murakami, A. Okuno, K. Inukai, T. Asano, Y. Kaburagi, K. Ueki, et al. 1999. Increased insulin sensitivity and hypoglycaemia in mice lacking the p85 alpha subunit of phosphoinositide 3-kinase. *Nat. Genet.* 21:230–235. http://dx.doi.org/10.1038/6023

Thomas, H.E., W. Irawaty, R. Darwiche, T.C. Brodnicki, P. Santamaria, J. Allison, and T.W. Kay. 2004. IL-1 receptor deficiency slows progression to diabetes in the NOD mouse. *Diabetes.* 53:113–121. http://dx.doi.org/10.2337/diabetes.53.1.113

Vomund, A.N., B.H. Zinselmeyer, J. Hughes, B. Calderon, C. Valderrama, S.T. Ferris, X. Wan, K. Kanekura, J.A. Carrero, F. Urano, and E.R. Unanue. 2015. Beta cells transfer vesicles containing insulin to phagocytes for presentation to T cells. *Proc. Natl. Acad. Sci. USA.* 112:E5496–E5502. http://dx.doi.org/10.1073/pnas.1515954112

Wen, L., R.E. Ley, P.Y. Volchkov, P.B. Stranges, L. Avanesyan, A.C. Stonebraker, C. Hu, F.S. Wong, G.L. Szot, J.A. Bluestone, et al. 2008. Innate immunity and intestinal microbiota in the development of Type 1 diabetes. *Nature.* 455:1109–1113. http://dx.doi.org/10.1038/nature07336

Wood, Z.A., E. Schröder, J. Robin Harris, and L.B. Poole. 2003. Structure, mechanism and regulation of peroxiredoxins. *Trends Biochem. Sci.* 28:32–40. http://dx.doi.org/10.1016/S0968-0004(02)00003-8

Wu, A.J., H. Hua, S.H. Munson, and H.O. McDevitt. 2002. Tumor necrosis factor-α regulation of CD4$^+$CD25$^+$ T cell levels in NOD mice. *Proc. Natl. Acad. Sci. USA.* 99:12287–12292. http://dx.doi.org/10.1073/pnas.172382999

Yamada, Y., Y. Okubo, A. Shimada, Y. Oikawa, S. Yamada, S. Narumi, K. Matsushima, and H. Itoh. 2012. Acceleration of diabetes development in CXC chemokine receptor 3 (CXCR3)-deficient NOD mice. *Diabetologia.* 55:2238–2245. http://dx.doi.org/10.1007/s00125-012-2547-8

Yang, X.D., R. Tisch, S.M. Singer, Z.A. Cao, R.S. Liblau, R.D. Schreiber, and H.O. McDevitt. 1994. Effect of tumor necrosis factor alpha on insulin-dependent diabetes mellitus in NOD mice. I. The early development of autoimmunity and the diabetogenic process. *J. Exp. Med.* 180:995–1004. http://dx.doi.org/10.1084/jem.180.3.995

Yosef, N., and A. Regev. 2011. Impulse control: temporal dynamics in gene transcription. *Cell.* 144:886–896. http://dx.doi.org/10.1016/j.cell.2011.02.015

Yosef, N., and A. Regev. 2016. Writ large: genomic dissection of the effect of cellular environment on immune response. *Science.* 354:64–68. http://dx.doi.org/10.1126/science.aaf5453

Yurkovetskiy, L.A., J.M. Pickard, and A.V. Chervonsky. 2015. Microbiota and autoimmunity: exploring new avenues. *Cell Host Microbe.* 17:548–552. http://dx.doi.org/10.1016/j.chom.2015.04.010

Zhao, X., A. Sato, C.S. Dela Cruz, M. Linehan, A. Luegering, T. Kucharzik, A.-K. Shirakawa, G. Marquez, J.M. Farber, I. Williams, and A. Iwasaki. 2003. CCL9 is secreted by the follicle-associated epithelium and recruits dome region Peyer's patch CD11b+ dendritic cells. *J. Immunol.* 171:2797–2803. http://dx.doi.org/10.4049/jimmunol.171.6.2797

SUPPLEMENTAL MATERIAL

Ferris et al., https://doi.org/10.1084/jem.20170074
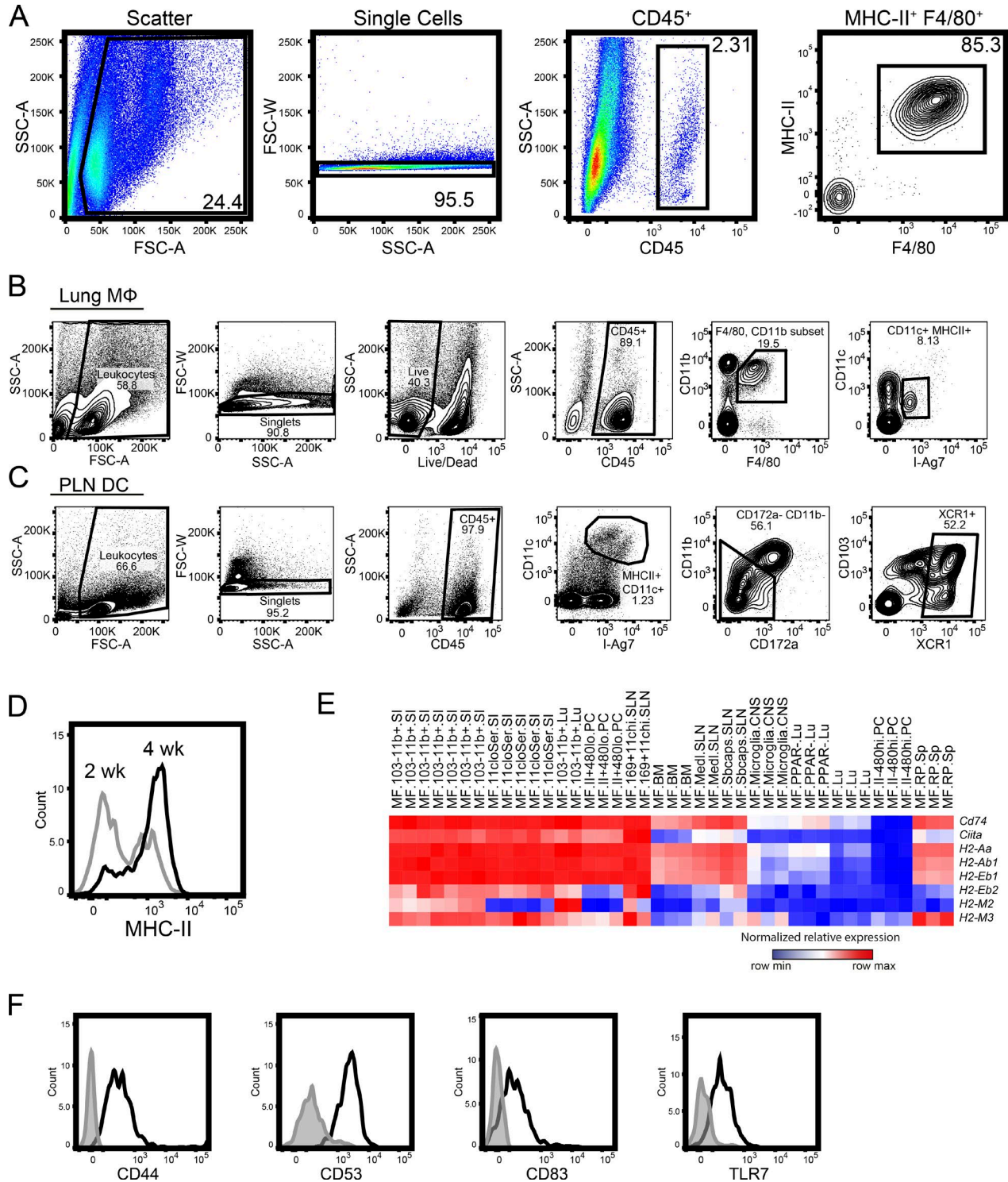
The Journal of Experimental Medicine

Figure S1.   **Analysis of islet macrophages.** (A) Flow cytometry gating strategy for sorting of macrophages from 3-wk-old mice. Cells were gated on the basis of forward and side scatter, single cells, CD45 expression, MHC-II, and F4/80 expression. Flow cytometry gating strategy of lung macrophages (B) and PLN XCR1^{+} DC (C) populations. Lung macrophages were gated on FSC/SSC, singlets, live dead, CD45, CD11c, F4/80, and MHC-II expression. XCR1^{+} DCs were gated on FSC/SSC, singlets, CD45, CD11c, MHC-II, CD11b, CD172a, CD103, and XCR1. (D) Expression of I-A[97] on CD45^{+} CD11c^{+} F4/80^{+} macrophages isolated from islets of 2-wk-old and 4-wk-old NOD female mice. (E) Expression of MHC-II complex genes, including the master regulator *Ciita* by different macrophage populations, on the basis of the ImmGen dataset (GSE15907). (F) Flow cytometry of CD45^{+} CD11c^{+} I-A[97+] NOD macrophages examining for CD44, CD53, CD83, and TLR7.
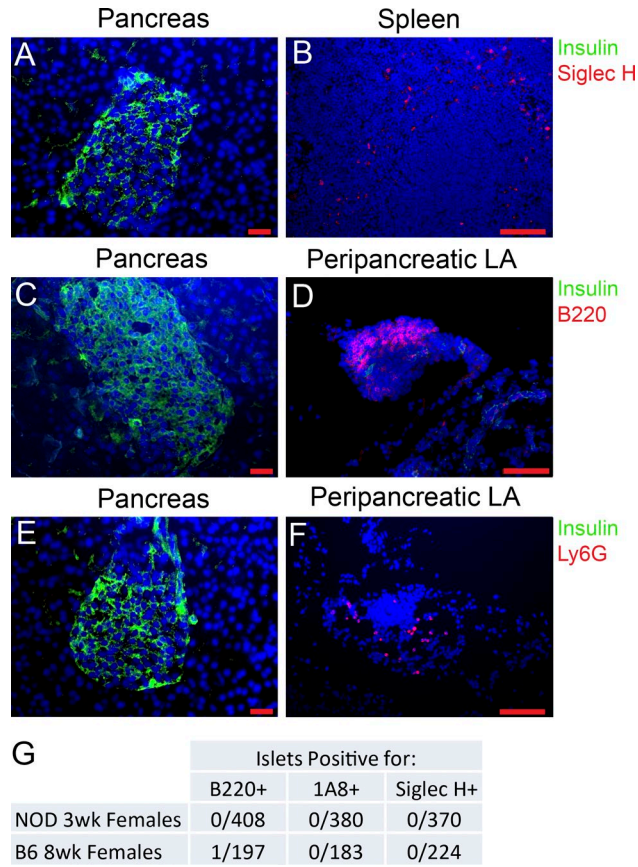
Figure S2. **Immunofluorescence of pancreas and lymphoid tissue.** (A, C, and E) Pancreatic sections and (B) splenic sections or (D and F) peripancreatic lymphoid aggregates (LA) were stained with anti-insulin (β cells) and (A and B) Siglec H (pDCs), (C and D) B220 (B cells), or (E and F) Ly6G (neutrophils). All sections were nuclear-stained with bisbenzimide. (G) The indicated number of islets were scored for the presence of either B220[+], 1A8 (Ly6G)[+], or SiglecH^{+} cells. Results were obtained from NOD mice at 3 wk and C57BL/6 mice at 8 wk of age (three mice for each).
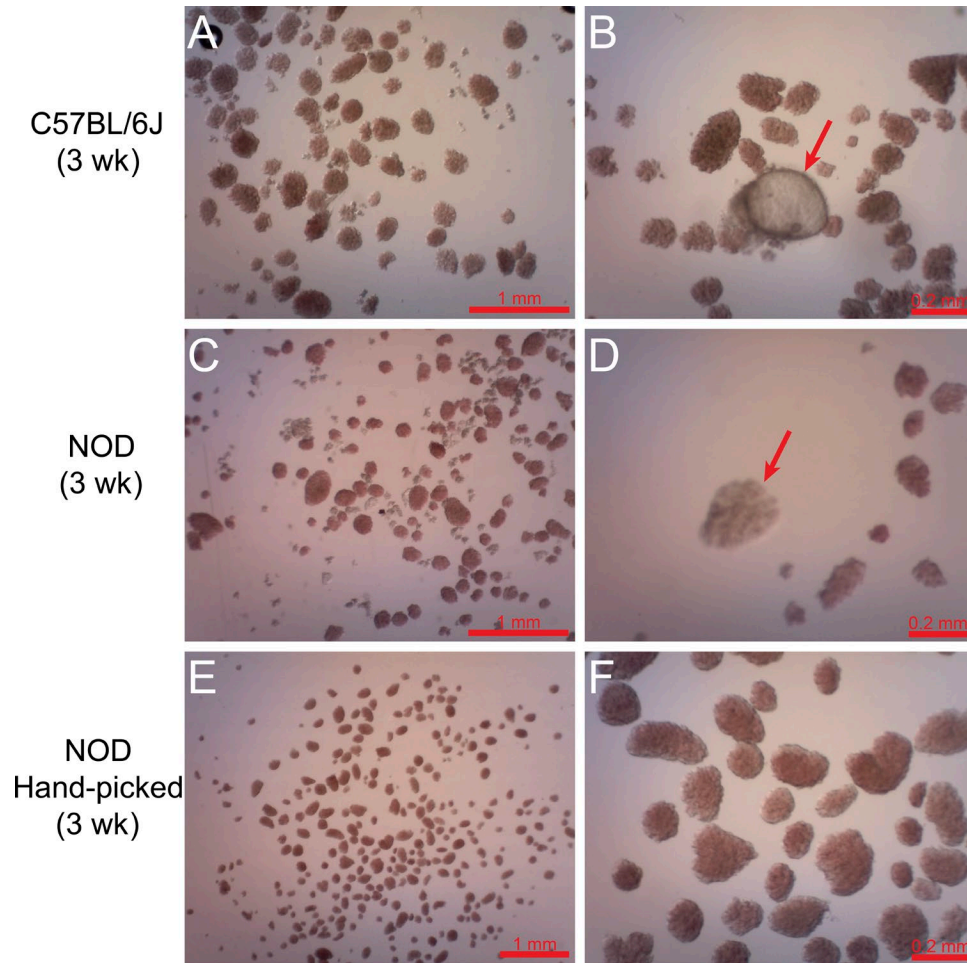
Figure S3. **Imaging of isolated islet preparations.** (A and B) C57BL/6J and (C and D) NOD pancreata were digested without hand picking and imaged. (E and F) NOD pancreata were digested, hand-picked under a dissection microscope, and imaged. All islet preparations were stained with dithizone to allow visual separation of islets from the acinar or lymphoid aggregate structures that associate with pancreas digestion preparations. Arrows indicate contaminating acinar or leukocytic aggregate structures.
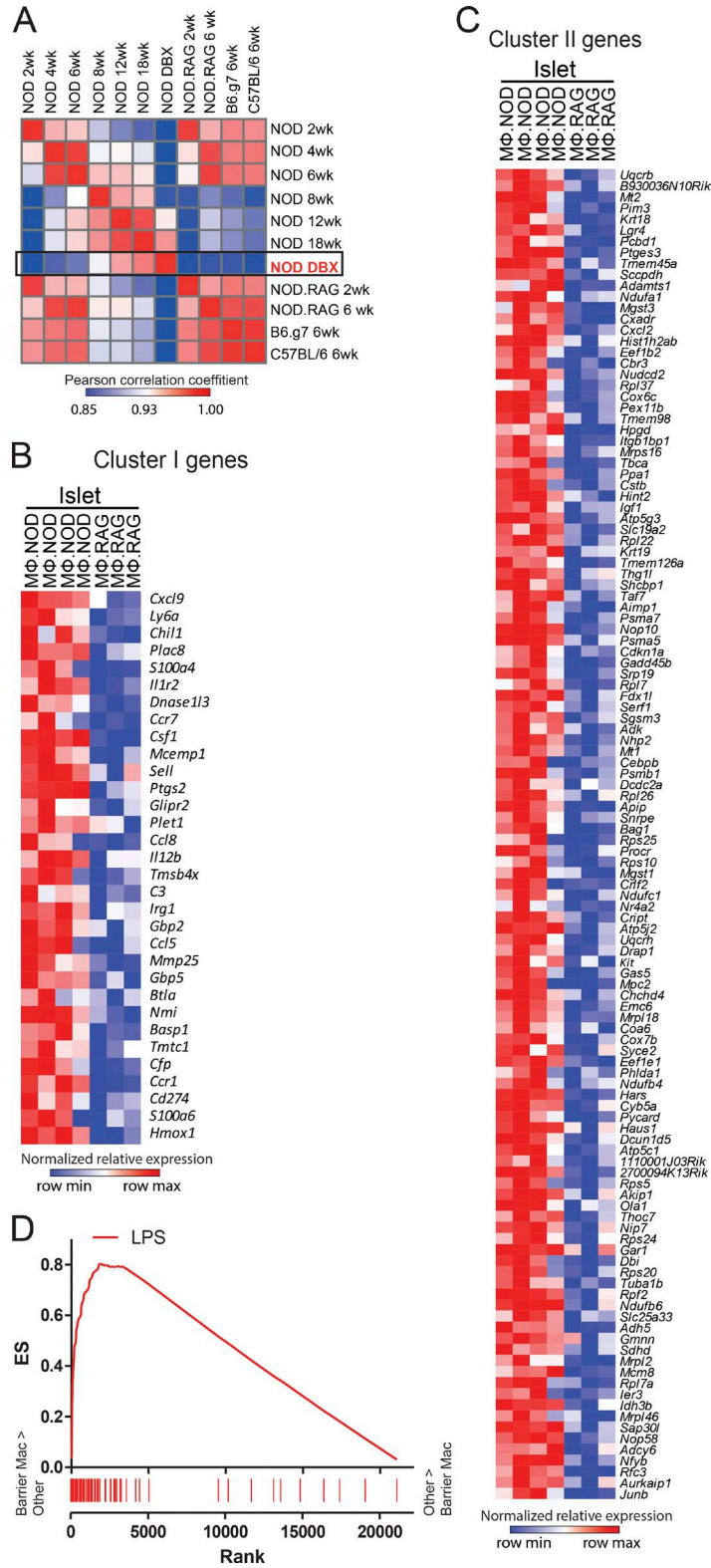
Figure S4. **There are two clusters of genes up–regulated in islet NOD macrophages compared with islet NOD.*Rag1*⁻/⁻ macrophages.** (A) Pearson's correlation between all samples on the basis of genes, differentially up-regulated in NOD versus NOD.*Rag1*⁻/⁻ islet macrophages with P ≤ 0.05, and maximum likelihood estimate–moderated fold change ≥2. Heat maps of (B) cluster I and (C) cluster II genes. (D) GSEA plots of lamina propria, serosal, and CD11b⁺CD103ⁿᵉᵍ lung macrophages comparing with other macrophages from ImmGen dataset, on the basis of LPS signature. ES, enrichment score.

Figure S5. **Heat map of single islet macrophage qRT–PCR data.** Single-cell qRT-PCR data for NOD and NOD.*Rag1*−/− macrophages were hierarchically clustered using Pearson's correlation. (A) Genes selected as significant in Fig. 7 B and (B) all genes were plotted by hierarchical clustering using Pearson's correlation for grouping and global Z score for scaling. The key on the bottom of the heat map indicates the cell type examined.

Table S1, included in a separate Excel file, is a gene expression table of islet and lung macrophages and NOD PLN DCs.